

Alma Mater Studiorum – Università di Bologna

DOTTORATO DI RICERCA IN
Meccanica e Scienze Avanzate dell'Ingegneria

Ciclo XXVIII

Settore Concorsuale di afferenza: 09/A2 – Meccanica Applicata alle Macchine

Settore Scientifico disciplinare: ING/IND-13 – Meccanica Applicata alle Macchine

SUBJECT SPECIFIC KNEE JOINT MODELLING BASED ON IN VIVO CLINICAL DATA

Presentata da: Fabrizio Nardini

Coordinatore Dottorato

**Chiar.mo Prof. Ing.
Vincenzo Parenti Castelli**

Relatore

**Chiar.mo Prof. Ing.
Vincenzo Parenti Castelli**

Esame finale anno 2016

Acknowledgements

At the end of a journey, there is a time when you sit down and look back to all the things passed. A PhD course is like a great and tough journey in which is easy to get lost. It would not be possible for me to arrive at the end this journey without the invaluable support of Professor Vincenzo Parenti Castelli. To him goes my deepest gratitude for his intellectual guidance, for his great support during all this years and for all the things he has taught to me. In italian "*insegnare*" ("*to teach*") means "to leave a mark", he surely did.

I also wish to thank Dr. Nicola Sancisi for his great help and his flawless advices during all the PhD course.

In the end, I'd like to thank Dr. Claudio Belvedere and Dr. Alberto Leardini at Istituto Ortopedico Rizzoli for providing the experimental facilities and for the help and the support throughout the research activity related to the following dissertation.

Contents

1	Introduction	1
2	Preliminaries	5
2.1	Anatomy of the knee	6
2.2	Appearance of the knee in medical imaging	8
2.3	Description of the motion: definition of the anatomical frames	10
3	Knee joint modelling	13
3.1	Kinematic model	14
3.1.1	The tibio-femoral mechanism	15
3.1.2	The patello-femoral mechanism	17
3.2	Stiffness model	20
4	From in vivo clinical data to the subject specific model	25
4.1	Data acquisition	26
4.1.1	Anatomical data	26
4.1.1.1	Bone models	26
4.1.1.2	Ligaments' insertion areas	29
4.1.1.3	Anatomical reference frames	30
4.1.2	Experimental passive motion	31
4.1.3	Clinical tests on the laxity of the knee	35
4.2	The identification of the subject specific model	36
4.2.1	First guess of the parameters	36
4.2.2	Optimization of the models parameters	39
4.2.2.1	Kinematic model	39
4.2.2.2	Stiffness model	43

4.3	Results and discussions	48
4.3.1	Kinematic model	48
4.3.2	Stiffness model	49
5	Conclusions	57
	References	61

1

Introduction

The knee is one of the most complex as well as one of the most thoroughly studied joint of the human musculoskeletal system. The reasons of the great attention devoted to it lie in the importance it has during daily living activities. Indeed, more than the other joints of the lower limb, it has to provide a wide range of motion together with the stability essential to sustain the upper part of the body. This two features, although contrasting, are the two key roles played by the knee joint. Moreover, the knee is one of the joints that undergoes the largest number of surgical treatments per year, not to mention the traumas and diseases that it suffers such as osteoarthritis. Therefore, a deep understanding of its behaviour and of the role played by each of the structures composing it, is fundamental in order to restore its physiological function.

Knee joint models are an invaluable tool to obtain a better understanding of the behaviour of the knee and their usefulness is proved in many fields. For instance, the increasing knowledge gained from models helps surgeons in surgical planning and in the treatment of joint related disorders, prosthetic and orthoses design takes advantage from the deeper comprehension of the function of motion guidance of the anatomical structures composing the knee as well. Finally, ligaments reconstruction greatly benefits from a careful knowledge of the knee joint stiffness.

A huge amount of models has been proposed in past and recent years [18, 19] trying to catch the behaviour of the knee joint from different point of view, several of them are focused on the kinematics and on the kinetostatic behaviour of the joint.

The kinematic models of the joint aims at the description of the joint passive motion; starting from the earlier planar descriptions of the knee motion like the Freudenstein-

1. INTRODUCTION

Woo model [9] or the four-bar linkage [43], researchers moved to more complex one degree of freedom equivalent spatial mechanisms [6, 34, 35, 39, 47], such as the equivalent spatial mechanisms.

In particular, within this family of mechanisms, there is one [34] that demonstrates great accuracy in replicating the knee joint passive motion combined with a high computational efficiency and the use of a small set of parameters to describe it. This mechanism, called 5-5 parallel mechanism, originates from experimental evidences that allow: (i) the consideration of particular fibres of ligaments (responsible of the guidance of passive motion together with the articular surfaces) as if they were links of constant length and (ii) the approximation of the condyle surfaces with spherical surfaces, so that the knee joint can be thought as kinematically equivalent to a 5-5 parallel mechanism whose five links mimics the guidance role of ligaments and articular surfaces.

Static and quasi-static models of the joint [5, 31, 41] focused on the stiffness of the knee trying to replicate the relative motion of the bones in different loading conditions and determine the forces generated in ligaments and articular contacts in order to satisfy the equilibrium conditions.

All the aforementioned models stem from data based on the literature or experiments carried out in vitro on cadaveric specimens. Currently in the literature there is a lack of in vivo subject specific models of the knee joint, the efforts in this direction are mainly focused on the evaluation of the joint loads in specific tasks or in the musculoskeletal modelling associated in particular with total knee arthroplasty [29] while almost neither kinematic nor kinetostatic models are found that are based on in vivo data.

The use of cadaveric specimens has several advantages: it allows an accurate reproduction and acquisition of the joint passive motion and a precise identification of all the anatomical structures composing the joint. However, models based on in vitro experiments suffer from an intrinsic lack of coherence. In fact, while on one hand in vitro procedures proved reliable and accurate in retrieving the data needed to define models of both the passive motion and the stiffness of the knee, on the other hand dynamic models including the loads of active structures (such as the forces exerted by muscles) cannot be defined properly in an in vitro context.

However, the identification of in vivo based models reveals some critical aspects and disadvantages with respect to its in vitro counterpart. For instance, the choice of

a suitable experimental set-up to correctly reproduce, acquire and measure the passive motion as well as the precise evaluation of the anatomical structures and their geometry are not easy goals to achieve in vivo.

In order to achieve a comprehensive knee joint description in which the kinematic, kinetostatic and dynamic models coherently stem one from the other, the identification of a procedure that allows to obtaining reliable kinematic and kinetostatic models in vivo is needed. Moreover, partly due also to the development of new technology like the 3-D printing, recently an increasing interest is growing towards the development of subject specific techniques that allows for the definition of customized models on a single patient. Therefore an in vivo knee joint model specialized on a specific subject is even more attractive.

In the present dissertation a procedure is defined that allows for the identification of a subject specific knee joint model in vivo starting from standard clinical data obtained by the use of non invasive techniques such as computed tomography (CT), magnetic resonance imaging (MRI) and fluoroscopy. This procedure leads to an accurate identification of the parameters needed to personalize the 5-5 parallel mechanism and its patello-femoral extension on a single patient in order to accurately reply the knee joint original motion. Furthermore, following the sequential approach to the modelling of the joint, a stiffness model of the knee [41] is specialized on the specific subject's anatomy.

In the next chapter a basic knowledge of the knee joint anatomy is reported together with a brief description of the appearance of the structures composing the joint in medical imaging and the convention adopted in the description of the knee motion. In the third chapter the kinematic and the stiffness models of the joint adopted in the dissertation are introduced and described. The fourth chapter is the core of the study. In the first part the procedure followed to identify the subject specific model of the joint starting from clinical data collected from CT, MRI and fluoroscopy is presented, then in the second the identification of the model parameters is described. Finally, the results of the identification process of the kinematic and of the stiffness models are shown and compared with the subject specific experimental motion and data from the literature.

1. INTRODUCTION

2

Preliminaries

The main purpose of the present chapter is to provide an overview of the anatomy of the knee joint. In particular, the chapter provides an introduction and description of the knee main structures. Moreover, this chapter is intended to make the reader familiar with the nomenclature used hereinafter in the dissertation.

For the sake of clarity, before going forward into the description of the knee anatomy, some fundamental terms are briefly introduced since they are extensively used in the following. Common practice in clinical environment is to locate the anatomical structures as well as to indicate the direction of movements with respect to anatomical planes (Fig. 2.1) thus defined:

- **Sagittal plane:** is a vertical plane (orthogonal to the ground), it divides the body into the right and left halves;
- **Coronal plane:** is a vertical plane (perpendicular to the sagittal plane), it separates the anterior from the posterior part of the body;
- **Transverse plane:** is an horizontal plane (perpendicular to the previous two), it divides the body into the inferior and the superior part.

Referring to Fig. 2.1, on the sagittal and the coronal planes the proximal-distal direction is defined by moving upwards (or downwards) from the centre of the body; similarly the medio-lateral direction is defined on the transverse and coronal planes by moving from the centre of the body to the left (or right), finally the anterior-posterior direction is defined on axial and sagittal planes by moving from the centre towards the anterior (or posterior) part of the body.

2. PRELIMINARIES

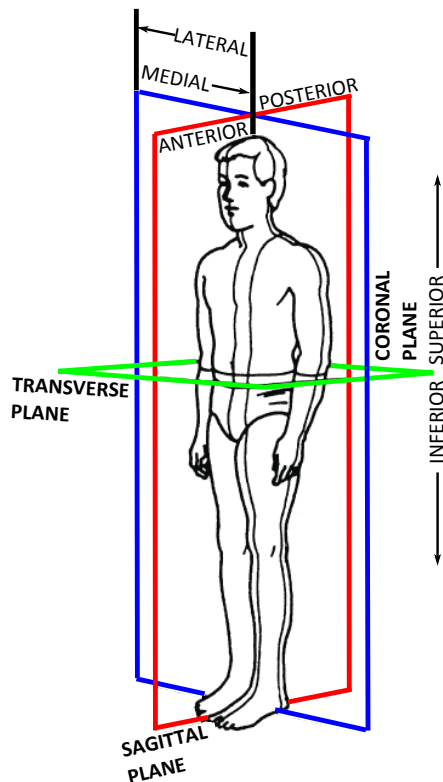


Figure 2.1: Anatomical planes and anatomical axes

2.1 Anatomy of the knee

The knee joint is the intermediate joint of the lower limbs, it is composed of three bones: the femur, tibia and patella. The distal segment of the femur articulates both with the proximal part of tibia and the patella, however this two bones never come in contact with each other. This feature leads to the subdivision of the knee joint into two sub-joints: the tibio-femoral (TF) and the patello-femoral (PF) joints.

In the first one, the medial and lateral condyles of the femur move on the tibial plateau (i.e. the tibial condyles); in-between the two, a couple of pads of fibrocartilaginous tissue called menisci are placed. As far as the PF joint is concerned, the back surface of the patella glides on the anterior surface of the condyles and on a grooved surface between them called trochlea.

A fourth bone, the fibula, is also mentioned in the following (although it does not belong to the knee joint directly) because of its connection to some fundamental

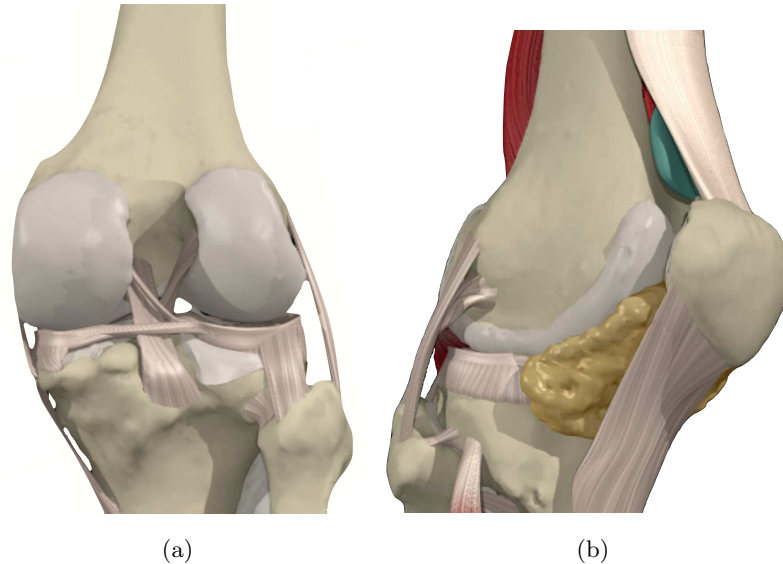


Figure 2.2: Antero-lateral and posterior view of the principal knee structures

structures of the knee. The fibula is placed on the postero-lateral side of the tibia, even though is not rigidly attached to it, their relative movement is strongly constrained.

Depending on the role, the different anatomical structures that compose the knee can be considered active or passive. Active structures, typically the muscles, are those that are able to produce forces; conversely the passive one can exert a force only if compressed or stretched by external factors, articular surfaces and ligaments are among this structures.

Muscles are not considered in this dissertation except for the quadriceps femoris. This muscle is the principal extensor muscle of the knee, it is subdivided into four different parts that originate from the ilium and the proximal part of the femur and are connected distally to the patella through the quadriceps tendon.

Articular surfaces are the portions of the bone that come in direct contact with other bones during the motion, in synovial joints (such as the knee) they are covered with a fibrous connective tissue called cartilage. In the knee those surfaces are the femoral and tibial condyles (in both cases subdivided in medial and lateral), the trochlea and the back surface of the patella.

Ligaments are fibrous structures composed of connective tissue mostly organized in bundles of fibers, they connect the articulating bones within a joint. The four primary

2. PRELIMINARIES

ligaments are the anterior cruciate ligament (ACL), the posterior cruciate ligament (PCL) and the two collaterals: the medial collateral ligament (MCL) and the lateral collateral ligament (LCL) (Figure 2.2 (a)). Particularly relevant is the subdivision of each one of the cruciate ligaments into two anatomically distinct bundles named after the position of their tibial insertion. The ACL is composed of an anteromedial (am-ACL) and a posterolateral (pl-ACL) bundle while the PCL is subdivided into an anterolateral (al-PCL) and a posteromedial (pm-PCL) bundles. The MCL is subdivided into a superficial bundle (sMCL) and a deep bundle (dMCL). Within the superficial bundle, a distinction similar to that of the cruciates is made distinguishing an anterior (ab-MCL) and a posterior (pb-MCL) bundles (when referring to the sub-bundles of the sMCL the prefix ‘s’ of the acronym is dropped in order to avoid to weigh down the notation). Furthermore, a fifth ligament, the patellar ligament (PL), that belongs to the PF joint and connects the anterior part of the proximal tibia is considered provided its importance for the PF joint (Figure 2.2 (b)).

Besides the aforementioned anatomical structures, other minor components are considered in the following, those are the structure that belongs to the postero-lateral and postero-medial part of the joint. In particular, from the postero-lateral corner of the knee the popliteus tendon (PT), the popliteofibular ligament (PFL) and the mid-third lateral capsular ligament (MLCL) are considered. The first one originates from a region near the lateral epicondyle and courses medially and distally on the posterior part of the knee until the posteromedial tibia where the popliteus muscle arise. The PFL originates from PT and inserts on the proximal part of the head of the fibula. The MLCL is a thickening of the lateral capsule of the knee, it originates near the lateral epicondyle and inserts in the lateral tibia. Among the structures that compose the postero-medial corner of the knee the posterior oblique ligament (POL) is included in the dissertation, it originates posterior to the origin of the sMCL on the femur and attaches on the posteromedial tibia. The role of these structures will be clarified in the following of the dissertation.

2.2 Appearance of the knee in medical imaging

In the following an overview of the appearance of the principal knee structures in MRI. This section is intended to provide a basic knowledge of knee anatomy from a medical

2.2 Appearance of the knee in medical imaging

imaging standpoint since it is essential for the purpose of the study. Particular relevance will be given to the description of both the anatomical structures and landmarks involved in the study as well as to the choice of the most suitable anatomical plane for each structure.

Ligaments generally appear on MRI as low signal intensity region (i.e. black). The ACL is visible in all standard anatomical planes [7] although for a careful evaluation of its bundles and origin/insertion areas the use of oblique coronal [44] or oblique axial [48] planes is suggested. If a coronal oblique plane is used, a plane parallel to the Blumensaat line (i.e. the border of the intercondylar notch as seen in the sagittal plane) is recommended. Coronal oblique planes allow the visualization of both the bundles in their development from the femur to the tibia, the am-ACL is reported to appear a homogeneous low signal intensity band while the pl-ACL shows less homogeneous than the am-ACL and hypointense (i.e. darker than the surrounding structures) around the tibia. The use of a axial oblique plane normal to the course of the ACL in the sagittal plane is also indicated in literature showing a better delineation of the bundles with respect to the standard anatomical planes [48]. In axial oblique planes near the tibial attachment the am-ACL is described to have a C-shaped hypointense border with a hyperintense (i.e. brighter than the surrounding structures) centre, close to the attachment to the femur the bundles are seen as hypointense region, with the pl-ACL being a little less hypointense than the am-ACL.

The PCL is visible in all planes and usually it is shown in its entire length in a couple of consecutive sagittal images; the femoral attachment site is well depicted in axial images, differently the tibial attachment is commonly visualized in the sagittal plane [7]. The two-bundle anatomy is indicated to be better visualized on axial planes.

Both the MCL and the LCL appear as homogeneous low-signal bands, on coronal images they are shown in their length, axial images are useful to discern the collaterals from the other posteromedial or posterolateral structures respectively [7, 28].

The posterior oblique ligament originates posterior to the MCL, axial images are useful to locate and differentiate it from this ligament, coronal oblique images appear to show the course of the POL as well as its distal attachment on the tibia [28].

Posterolateral corner structures such as the popliteofibular ligament proves difficulty to visualize on in vivo MRI, oblique coronal images parallel to the longitudinal axis of PT are suggested to enhance its visualization [7]. On the contrary, the PT

2. PRELIMINARIES

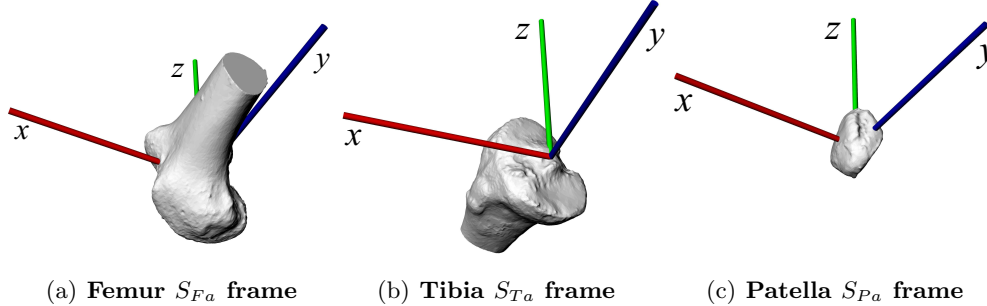


Figure 2.3: The anatomical frames of femur, tibia and patella: the red one is the antero-posterior (x) axis, the blue one is the proximal-distal (y) axis, the green one is the medio-lateral (z)

is easily identifiable from coronal and sagittal images whereas the axial plane is not recommended due to magic angle artefact (i.e. a brightening effect that affects the structures with ordered collagen fibres in a specific direction which form a particular angle with the magnetic field).

As far as the MLCL there are no particular prescription in literature concerning a preferred plane for the visualization as far as the author knows, in the present study, due to the uncertainty in its identification from imaging, its attachment areas are located by means of literature data dealing with its position with respect to bony landmarks.

2.3 Description of the motion: definition of the anatomical frames

In order to describe the knee motion as well as to locate the structures connected to each bone, the definition of the reference systems attached to the femur, tibia and patella is needed; these will be called anatomical frames (or anatomical reference systems) hereinafter. The relative motion of the fibula with respect to the tibia is not considered in this study.

The frames are chosen in accordance with the recommendations of the International Society of Biomechanics (ISB) [49] aiming at the clinical relevance of the joint motion description. Moreover, all of them are defined by means of anatomical landmarks easily recognizable through palpation or medical imaging.

The femur anatomical frame (S_{Fa}) is defined as follow (Fig. 2.3 (a)):

2.3 Description of the motion: definition of the anatomical frames

- the origin placed in the midpoint between the medial and lateral epicondyles;
- the x-axis orthogonal to the plane defined by the two epicondyles and the centre of the head of the proximal part of the femur, anteriorly directed;
- the y-axis parallel to the line joining the origin with the centre of the head of the femur;
- the z-axis directed according to the right hand rule.

Similarly, the tibial anatomical frame (S_{Ta}) is obtained as follow (Fig. 2.3 (b)):

- the origin coincident with the deepest point between the tubercles of the intercondylar eminence;
- the x-axis orthogonal to the plane identified by the two malleoli and the origin, anteriorly directed;
- the y-axis parallel to the line joining the midpoint between the malleoli and the origin;
- the z-axis directed according to the right hand rule.

Likewise, the patella anatomical frame (S_{Pa}) is defined with (Fig. 2.3 (c)):

- its origin coincident with the mid point between the medial and lateral apices;
- the x-axis normal to the plane defined by the aforementioned apices and the distal one;
- the y-axis parallel to the line joining the distal apex to the origin;
- the z-axis directed according to the right hand rule.

To comply with the clinical description of the motion adopted, the orientation of the femur and patella relatively to tibia and femur respectively is described by means of the Grood & Suntay joint coordinate system [14]. To wit, a joint reference frame is defined for each one of the two sub-joint using two body fixed axes (one for each bone) and a third floating axis mutually orthogonal to the first two. Accordingly, the TF joint reference system is composed by the z-axis of S_{Fa} , the y-axis of S_{Ta} and

2. PRELIMINARIES

a third axis perpendicular to the previous ones. The orientation of the femur with respect to the tibia is parametrised by means of three angular coordinates expressing the rotations around these axes: the flexion/extension α , the ab/adduction β and the intra/extra rotation γ respectively. Positive signs of α , β , γ correspond to femoral flexion, abduction and external rotation.

With the use of the aforementioned joint frame, the relative pose of the femur with respect to the tibia is identified by the position vector \mathbf{p}_{tf} of the origin of S_{Fa} in S_{Ta} and the matrix $\mathbf{R}_{tf} \in SO(3)$ function of α , β and γ :

$$\mathbf{R}_{tf} = \begin{bmatrix} c_\alpha c_\gamma + s_\alpha s_\beta s_\gamma & -s_\alpha c_\gamma + c_\alpha s_\beta s_\gamma & -c_\beta s_\gamma \\ s_\alpha c_\beta & c_\alpha c_\beta & s_\beta \\ c_\alpha s_\gamma - s_\alpha s_\beta c_\gamma & -s_\alpha s_\gamma - c_\alpha s_\beta c_\gamma & c_\beta c_\gamma \end{bmatrix} \quad (2.1)$$

where c and s stand for sine and cosine, the subscripts indicate the argument of the function. It is worth noting that the relation is for a right leg, in case of a left one, the sign of β and γ should be changed. The joint reference system for the patello-femoral joint is defined in the same way with the z-axis of S_{Pa} , the y-axis of S_{Fa} and their common perpendicular. The pose of the patella relatively to the femur is given by the position vector \mathbf{p}_{fp} of the origin of S_{Pa} in S_{Fa} and the matrix $\mathbf{R}_{fp} \in SO(3)$ for which a relation similar to Eq. (2.1) holds.

3

Knee joint modelling

The knee is one of the most complex and studied joint of the human body provided its great importance in locomotion, for this reason a huge amount of models have been proposed in the literature.

Mainly, knee joint models can be subdivided into two categories according to the approach chosen in studying its behaviour: the ‘simultaneous’ approach based models and the ‘sequential’ approach based ones [41]. In the first one, all the knee structure (both active and passive) are considered at once, trying to fit the behaviour of the joint during a particular task. This approach surely guides to the identification of a set of parameters that allow for a good fitting of the chosen task, but the validity of the identified set of parameters is limited only to that particular task and the predictive potential of a general and different task is not guaranteed.

On the contrary, the sequential approach builds up the model step by step starting from a first simple model that is consequently enriched relaxing the hypotheses on which is based. That is, the construction of the model is subdivided into consecutive steps, each one of which is a model in itself and constitutes a generalization of the previous. At every step, only the anatomical structures that affect the development of the motion in the considered loading condition are introduced besides those defined in the steps before, so that only a group of structure is identified per step. It is important in this approach to make sure that the generalization process from a simple model towards more sophisticated ones preserves the behaviour of each model of the sequence. Thus, every model has to replicate the behaviour of the previous, provided that it is placed

3. KNEE JOINT MODELLING

in the same loading condition. This leads to two rules to follow in order to ensure that [41]:

1. A parameter identified at one step, is not modified in the following;
2. The parameters introduced at every step have not to alter the behaviour of the models defined at previous steps.

This process of consecutive generalization leads to the definition of a completely general knee model able to describe the joint behaviour in different task related to different loading conditions and allows for a better understanding of the role of each structure. For these reasons, in the present dissertation the sequential approach is followed. As a first step of the sequential procedure a subject specific kinematic model of the knee is defined, on top of this, the stiffness model defined in the second step will stand.

3.1 Kinematic model

A good starting point for the built up process is the passive motion, that is to say the motion of the knee joint when no loads are applied to it (neither internal forces exerted by muscles nor external ones). For its nature, it surely represents a favourable place to start with, since it is the simplest loading condition at hand.

The kinematic model of the knee joint passive motion adopted in this study, proposed in [33, 40], stems from experimental evidences on the behaviour of the structures that compose the joint and accurately represents its motion by means of an equivalent spatial mechanism. This model is complete both of the tibio-femoral and of the patello-femoral joints and is composed of one sub-chain per sub-joint. The two sub-chain are partially decoupled since the motion of the of the TF joint is not affected by the PF one, so that the two joints can be studied and modelled separately. The reason lies in the fact that the patella slides on the anterior surfaces of femur condyles and on the trochlea being connected to the femur via the quadriceps femoris (which in passive motion does not exert force on it) and to the tibia by means of PL ligament. During passive motion the patella is dragged by this ligament and its pose is determined by the pose of the TF joint and the geometry of the aforementioned surfaces given that the quadriceps femoris is not tight and does not impose restraints to the patellar motion.

Therefore the TF sub-chain works independently from the PF ones in accordance with the natural behaviours of the two sub-joints.

In the following the TF and the PF mechanisms are described with particular attention to the experimental evidences on which are based and their mathematical foundations are detailed.

3.1.1 The tibio-femoral mechanism

The model adopted in the present dissertation for the TF joint was firstly presented in [34] and originates from a set of one degree of freedom (DoF) parallel mechanisms proposed to reproduce the motion of the human knee. This model in particular represents an optimal trade off between accuracy and computational expensiveness.

The model relies on experimental evidences on the behaviour of the structures of the knee during passive motion. Several studies show that the passive motion of the knee is a 1-DoF spatial motion in which all the components of the movement are coupled with the flexion angle [46]. Moreover, experimental evidences show that fibres are identifiable within the ACL, PCL and the superficial MCL ligaments that remains almost isometric during the passive motion [4, 10, 11, 38]. Differently, neither other bundles (either within these ligaments or in other ligaments) nor muscles (which, not exerting forces, are relaxed) result tight during passive motion. These observations lead to recognize the isometric fibres of the cruciates and of the superficial medial collateral ligament and the geometric constraints imposed by the articular surfaces as the responsible of the guidance of the passive motion.

On the basis of the aforementioned consideration, the isometric fibres of ACL, PCL and sMCL are modelled as binary rigid link connecting the tibia and the femur through spherical pairs since their length does not change during the passive motion. As far as the articular surfaces are concerned (i.e. the medial and lateral condyles of femur and tibia) they are rendered with two couples of spheres rolling and sliding one on the other. Assuming the articular surfaces as infinitely rigid, the two superior pairs given by the four spheres can be substituted with binary rigid links connecting the centres of each couple of spheres by means of spherical pairs (this is possible because, within this hypothesis, the contact between the spheres is punctual). It is easy to recognize a 5-5 parallel mechanism as the final kinematic model of the tibio-femoral joint, with the tibia and the femur being the base and the platform respectively, and the passive

3. KNEE JOINT MODELLING

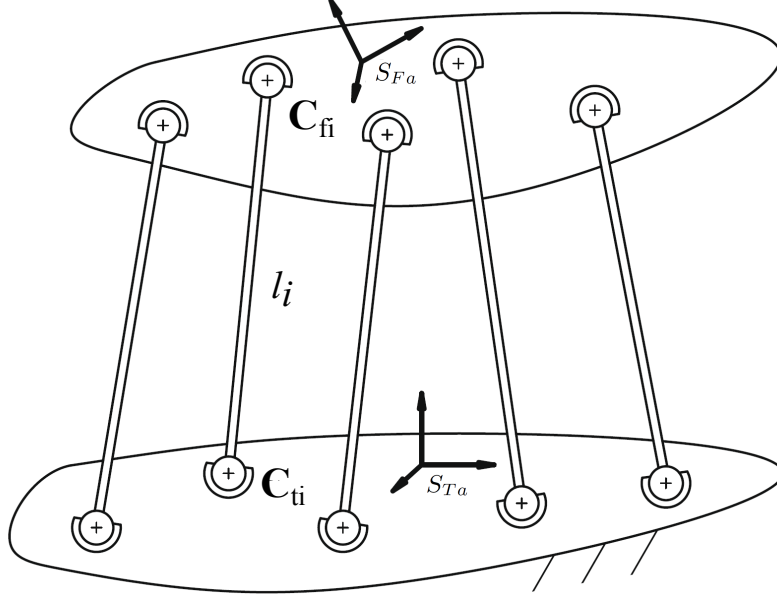


Figure 3.1: The 5-5 parallel mechanism

structures (i.e. the ligaments and the articular surfaces) acting as the binary rigid links of the mechanism (Fig. 3.1).

The anatomical reference systems S_{Ta} and S_{Fa} (see section 2.3) are used to describe the orientation of the tibia and the femur. Since the tibia is supposed fixed, S_{Ta} is elected as the global reference system. The transformation of the representation of a vector from S_{Fa} to S_{Ta} is done as explained in section 2.3 using the rotation matrix \mathbf{R}_{tf} and the vector \mathbf{p}_{tf} .

The closure equation of the aforementioned equivalent parallel mechanism are obtained imposing for each link the euclidean distance between the centre of the spheres to be equal to the length of the link:

$$\|\mathbf{c}_{ti} - \mathbf{c}_{fi}\| = l_i \quad \text{for } i = 1, 2 \dots 5 \quad (3.1)$$

where \mathbf{c}_{ti} and \mathbf{c}_{fi} (both represented in S_{Ta}) are the centre of the spherical pairs of the binary link on tibia and femur respectively and l_i is the length of each link. The geometry of the tibio-femoral joint is thus defined by 35 scalar values: the positions of the centres of the spherical pairs and the lengths of the links.

Given that the flexion angle α is the only DoF of the mechanism, the position and orientation of the joint is completely defined for an assigned value of the flexion angle.

For a given α , the equations (3.1) defines a system of five equations in five unknowns: the angles β , γ and the components of the vector \mathbf{p}_{tf} (introduced in section 2.3). Its solution allows for the determination of the pose of the femur with respect to the tibia.

3.1.2 The patello-femoral mechanism

The patello-femoral mechanism stems from considerations similar to those done for the TF joint. Throughout almost the whole range of knee flexion-extension, the dorsal surface of the patella slides on the articular surfaces of the femur (namely the trochlea and the anterior part of the condyles). Several studies [17] reveal that the mating surfaces of the femur and the patella maintain contact on a broad area during the passive flexion-extension. As a consequence their contact can be modelled as a lower pair, in particular the anterior articular surfaces of the femoral condyles can be modelled with a cylindrical surface. In addition, the patellar motion is deeply influenced by the shape of the trochlear groove [1] which is not orthogonal to the longitudinal axis of the aforementioned cylinder causing the patella to exhibit a nearly helicoidal motion. Moreover, experimental evidences [4] highlight the existence of isometric fibres within the patellar ligament (like the cruciates and the collaterals in the TF joint) that drag the patella during the passive motion. From all the previous observation the importance of the passive structures in the guidance of the motion of the patella is clear: the joint action of the isometric fibres of the patellar ligament and the geometry of the articular surfaces define the patellar motion throughout the flexion arc of the knee.

Taking advantage from these observation, a model of the PF joint was proposed [40] in which the articular surfaces were modelled as a screw joint and a binary rigid link connected to the tibia and the patella by means of spherical pairs models the isometric fibres of the patellar ligament.

In order to complete the kinematic model of the joint, it is necessary to consider a parameter to set the configuration of the joint for a fixed flexion angle. In physiological condition this task is fulfilled by muscles, precisely it is accomplished by the quadriceps femoris. Its action can be mimicked by two rigid binary links with a prismatic pairs in-between and connected to the ileum and the patella with spherical pairs. This group fixes the the configuration of the joint through the axial translation of the prismatic joint (see Figure 3.2 (a)). It is worth noting that for a given configuration of the TF sub-chain, the PF sub-chain has zero degrees of freedom so that its configuration is

3. KNEE JOINT MODELLING

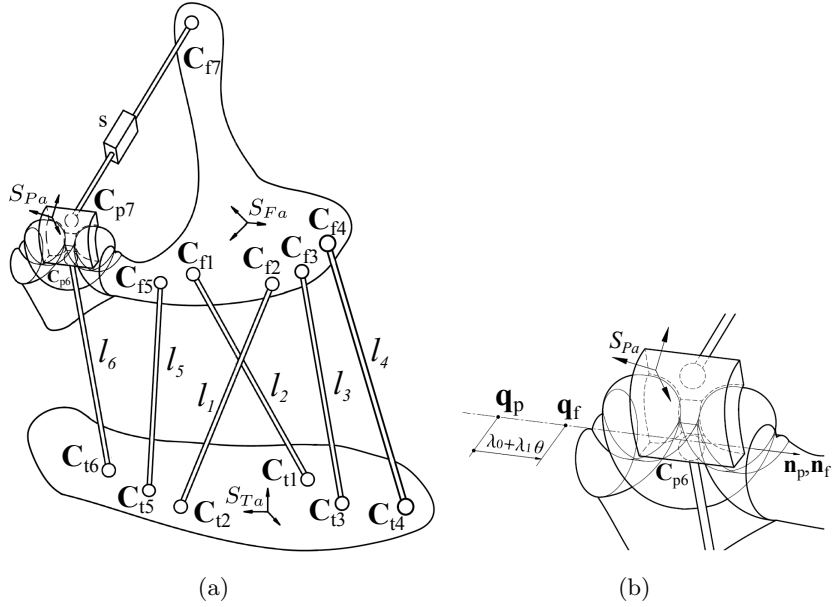


Figure 3.2: The 5-5 parallel mechanism complete with the PF sub-chain. A detailed view of the PF joint is showed together with its geometrical parameters.

completely defined by the position and orientation of the TF chain in accordance with the experimental evidences on the behaviour of the patello-femoral joint.

As far as the mathematical description of the screw pair is concerned, its axis is defined on the femur by the unit vector \mathbf{n}_f and the point \mathbf{q}_f (both represented in S_{Fa}) and, on the patella, by \mathbf{n}_p and \mathbf{q}_p (both represented in S_{Pa}) (Figure 3.2 (b)). The translation of the patella along the longitudinal axis of the cylinder is given by the two scalar parameters λ_0 and λ_1 : the first one identifies the distance between \mathbf{q}_p and \mathbf{q}_f in the reference position, the second one sets the translation between the two points along the axis related to 1 radian of rotation of the patella with respect to the femur.

With the use of the anatomical reference frames and the convention described in section 2.3; assigned the frames S_{Pa} to the patella and S_{Fa} to the femur, the relative pose of the patella with respect to the femur is given by the rotation matrix \mathbf{R}_{fp} and the vector \mathbf{p}_{fp} , thus resulting as a function of the angles α , β , γ and of the components of the vector \mathbf{p}_{fp} . Similarly, the position and orientation of the femur with respect to the tibia is given by the rotation matrix \mathbf{R}_{tf} and the vector \mathbf{p}_{tf} as explained in the previous section and in section 2.3.

Like for the tibio-femoral mechanism, the patello-femoral relative motion can be

obtained solving the closure equation of the mechanism for every flexion angle:

$$\begin{aligned}
 \mathbf{R}_{fp}\mathbf{n}_p &= \mathbf{n}_f \\
 \mathbf{R}_{fp}\mathbf{q}_p + \mathbf{p}_{fp} &= (\lambda_0 + \lambda_1\theta)\mathbf{n}_f + \mathbf{q}_f \\
 \|\mathbf{R}_{tf}(\mathbf{R}_{fp}\mathbf{c}_{p6} + \mathbf{p}_{fp}) + \mathbf{p}_{tf} - \mathbf{c}_{t6}\| &= l_6
 \end{aligned} \tag{3.2}$$

where \mathbf{c}_{p6} (represented in S_{Pa}) and \mathbf{c}_{t6} (represented in S_{Ta}) are the centres of the spheres of the rigid link that connects the patella with the tibia and l_6 its length, \mathbf{q}_p is represented in S_{Pa} while \mathbf{q}_f in S_{Fa} . The angle θ is the rotation of the patella around the axis of the joint with respect to the reference pose, it is given by:

$$\theta = \arcsin\left(\frac{r_{21} - r_{12}}{2n_{pz}}\right) \tag{3.3}$$

where r_{12} and r_{21} are elements of the transformation matrix of the vector components between the actual position and the reference pose (the first index stands for the rows while the second indicates the columns), n_{pz} is the component along the z axis of S_{Pa} . The first two equations of the system (3.2) impose the axis of the cylinder as represented in S_{Fa} to coincide with its representation in S_{Pa} , the third one fixes the distance of the spherical pairs to be equal to the length l_6 . In Eq. (3.2) \mathbf{R}_{tf} and \mathbf{p}_{tf} are knowns and given by the solution of Eq. (3.1), the only unknowns are the angles α , β and γ relative to the PF joint and the components of \mathbf{p}_{fp} . As a consequence, Eq. (3.2) is a system of 7 equations in 6 unknowns. However, only two out of the three scalar equations composing the first vectorial equation of Eq. (3.2) are independent since \mathbf{n}_p and \mathbf{n}_f are unit vectors.

Seventeen scalar values are needed to identify the geometry of the model: the coordinates of the centres of the two spherical pairs (\mathbf{c}_{p6} and \mathbf{c}_{t6}), the unit vectors of the axis of the cylinder (\mathbf{n}_p and \mathbf{n}_f), the points \mathbf{q}_p and \mathbf{q}_f and the two scalar values λ_0 and λ_1 . Only two scalar parameters are needed to define the vectors \mathbf{n}_p and \mathbf{n}_f since their norm is unitary. Indeed, defining α the angle between \mathbf{n}_p (or \mathbf{n}_f) and the z -axis of S_{Pa} (S_{Fa}) and β the angle between the projection of \mathbf{n}_p (or \mathbf{n}_f) on the xy plane and the x -axis of the same reference system, the aforementioned unit vectors can be

3. KNEE JOINT MODELLING

expressed as:

$$\begin{aligned}\mathbf{n}_p &= \begin{pmatrix} \cos \alpha_p \sin \beta_p \\ \sin \alpha_p \sin \beta_p \\ \cos \beta_p \end{pmatrix} \\ \mathbf{n}_f &= \begin{pmatrix} \cos \alpha_f \sin \beta_f \\ \sin \alpha_f \sin \beta_f \\ \cos \beta_f \end{pmatrix}\end{aligned}\tag{3.4}$$

Similarly, also the definition of the points \mathbf{q}_p and \mathbf{q}_f requires only two parameters each (namely their x and y coordinates) given that their position on the axis of the cylinder is arbitrary.

As previously said, the group composed by the prismatic pair and the two binary rigid links that model the action of the quadriceps femoris do not appear in the equation provided that the parameter s of the prismatic pair varies according to the current configuration of the PF joint in order to set the distance between \mathbf{c}_{p7} and \mathbf{c}_{f7} (i.e. the length of the quadriceps) and does not affect the motion.

3.2 Stiffness model

According to the sequential approach, the stiffness model stems directly from the kinematic one previously introduced. In this second step the model inherits the features of the previous model but relaxes the constraint on the description of the passive structures. In fact, while in the kinematic model the fibres of the ligaments and the articular contacts are modelled as rigid links, in the stiffness one the passive structures are treated as deformable elements able to exert forces when stretched or compressed. In this step of the sequential procedure, in order to determine the stiffness of the passive structures of the knee as well as the unloaded length of the ligaments fibres, the motion of the knee joint is considered when static external loads are applied to it. Like the previous step, the contribution of the active structures (i.e. the muscles forces) is not considered.

The model proposed in [41] is chosen since it proved to be reliable and accurate. In its formulation ligaments are modelled as elastic elements using a multi-fibre approach. Every ligament is subdivided into several bundles according to evidences on its own anatomical appearance. Each bundle is represented by a number of elastic elements depending on its shape and dimension [31, 32]. Each ligament considered in the model is thus composed of the fibres related to the bundles taken into account (depending on

the ligament) plus the isometric fibres defined at the previous step of the sequential procedure. Like the isometric fibres, also the articular contacts come as defined in the kinematic model, both of them are treated as elastic elements. Every elastic element is considered as a straight line element connecting the insertion points on tibia and femur, therefore the interaction between the fibres and the bone as well as the possible collisions between the fibres are not considered.

The tensile force f_i generated in a passive structure is related to the strain by means of a quadratic law [31], the relation is a piecewise function given that both the ligaments and the articular contacts exert force only when stretched (ligaments) or compressed one on the other (articular contacts). For ligaments the force exerted reads:

$$\begin{aligned} f_i &= k_i \epsilon_i^2 & \text{if } \epsilon_i > 0 \\ f_i &= 0 & \text{if } \epsilon_i \leq 0 \end{aligned} \tag{3.5}$$

The strain of the fibres ϵ_i that appears in Eq. (3.5) is defined as:

$$\epsilon_i = \frac{l_i - l_{i0}}{l_{i0}} \tag{3.6}$$

where l_i is the actual length of the fibre and l_{i0} is the zero-load length of the ligament, viz the ultimate length at which the ligament still does not exert force. The relation of Eq. (3.5) holds identically also for the articular contact of tibial and femoral medial condyles since they are both convex. Differently, it has to be slightly changed for the lateral articular contact since it occurs between a concave surface (tibial lateral condyle) and a convex one (the lateral condyle of the femur). In this case the Eq. (3.5) modifies in:

$$\begin{aligned} f_i &= -k_i \epsilon_i^2 & \text{if } \epsilon_i < 0 \\ f_i &= 0 & \text{if } \epsilon_i \geq 0 \end{aligned} \tag{3.7}$$

The difference between Eq. (3.5) and Eq. (3.7) is easy to understand with the aid of Fig. 3.3. Differently to the ligaments that exert forces when stretched, the articular contacts originate a constraint force that prevents the penetration of the surfaces. On the medial side of the knee both the femoral condyle and the tibial plateau have convex surfaces so that they come in contact when the distance between the endpoints of the spring increases (see Fig. 3.3 (b)). On the contrary, on the lateral side, the concave shape of the tibial plateau cause the surfaces to come in contact when the distance between the endpoints of the spring decreases (see Fig. 3.3 (a)).

3. KNEE JOINT MODELLING

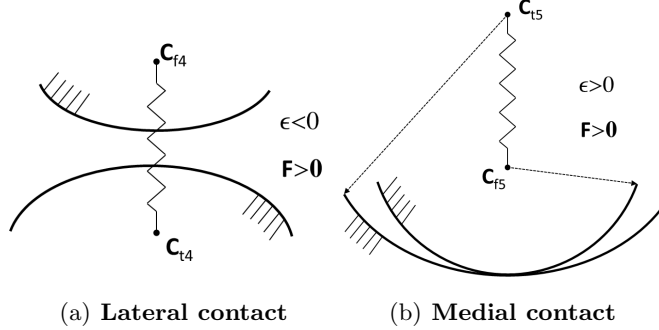


Figure 3.3: Model of medial and lateral contacts: effect of the curvatures of the surfaces.

The static equilibrium configuration is sought solving the equilibrium equations at every flexion angle. The femur is considered the fixed body while the tibia is considered the moving one, its pose is given with the use of convention described in section 2.3. Several loads are applied to the tibia: the external force \mathbf{F}_e or couple \mathbf{M}_e (according to the loading condition, as explained in the forthcoming chapter), the force due to its own weight plus the weight of the foot \mathbf{F}_w and the forces coming from ligaments' fibres \mathbf{F}_i . For the last ones, the following relations holds:

$$\mathbf{F}_i = f_i \frac{\mathbf{p}_{fi} + \mathbf{R}_{tf}^T (\mathbf{p}_{tf} - \mathbf{p}_{ti})}{l_i} \quad (3.8)$$

$$l_i = \|\mathbf{p}_{fi} + \mathbf{R}_{tf}^T (\mathbf{p}_{tf} - \mathbf{p}_{ti})\|$$

where \mathbf{p}_{fi} and \mathbf{p}_{ti} are the coordinates of the fibres insertion points on femur and tibia expressed in S_{Fa} and S_{Ta} respectively, f_i is the module of the force exerted by the ligament (as previously explained), l_i is the length of the ligament.

With the notation previously defined, the equilibrium for forces and moments acting on the tibia reads:

$$\sum_{i=1}^n \mathbf{F}_i + \mathbf{F}_e + \mathbf{F}_w = \mathbf{0} \quad (3.9)$$

$$\sum_{i=1}^n \mathbf{M}_{O_i} + \mathbf{M}_e + \mathbf{M}_{O_e} + \mathbf{M}_{O_w} + \mathbf{M}_c = \mathbf{0}$$

where \mathbf{M}_{O_i} , \mathbf{M}_{O_e} and \mathbf{M}_{O_w} are the moments of \mathbf{F}_i , \mathbf{F}_e and \mathbf{F}_w with respect to an arbitrary pole \mathbf{O} , \mathbf{M}_c is the balancing moment applied to fix the flexion angle and n is total number of ligaments' fibres included in the model. Equations (3.9) define system

3.2 Stiffness model

of six scalar equations in six unknowns whose resolution leads to the determination of the pose of tibia with respect to the femur at every flexion angle.

3. KNEE JOINT MODELLING

4

From in vivo clinical data to the subject specific model

The present chapter describes the procedure followed in order to define the subject specific model starting from in vivo clinical data. The procedure is subdivided into two parts: the in vivo acquisition of data and the identification of the knee joint model parameters. Figure 4.1 summarizes the workflow followed to define the subject specific model starting from in vivo clinical data.

The procedure for the acquisition of the data is further composed of several parts:

1. The starting point is given by the medical imaging techniques: the subject's anatomy is acquired by means of CT scan and MRI, a fluoroscopy allows for the passive motion to be recorded.
2. The data acquired from CT and MRI are processed. The three-dimensional bone models based on CT and MRI images are created. From the MRI based model the articular surfaces are extracted. The insertion areas of the ligaments are segmented on the images of the MRI in order to define the insertion areas.
3. The knee joint motion is obtained by matching the CT based models on the images acquired through fluoroscopy.

The identification of the model's parameters is based on the acquired data and is done by means of optimization processes aimed at refining the acquired data trying to fit the knee joint behaviour.

4. FROM IN VIVO CLINICAL DATA TO THE SUBJECT SPECIFIC MODEL

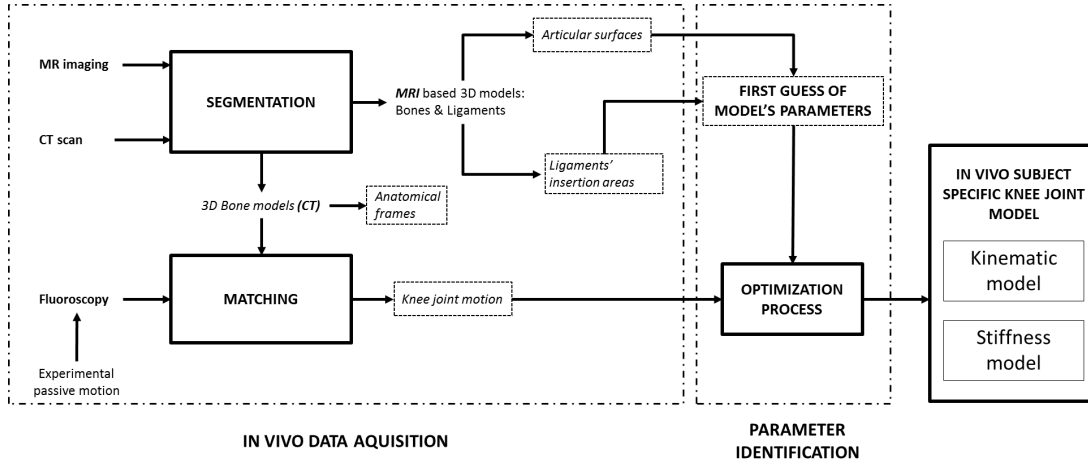


Figure 4.1: The workflow for the identification of the subject specific model.

4.1 Data acquisition

4.1.1 Anatomical data

In order to collect the data required for the model, medical tests and an experimental session were carried out at the Istituto Ortopedico Rizzoli with the technical and scientific assistance of the Movement Analysis Laboratory and the Radiology laboratory.

A voluntary subject (66 years old, male, 169 cm, 58 kg) was selected for the study provided that he was not suffering of any knee joint disease at the time of the study nor he had history of any knee related disorders.

Medical tests were needed to acquire the data related to the subject anatomy useful as a first approximation of the model's geometry, an experimental session allowed for the passive motion of the knee joint to be acquired.

4.1.1.1 Bone models

As far as the anatomical data are concerned, the shape of the different bony segments were obtained by means of CT scan (Philips, Brilliance 16). The subject was asked to lay down supine on the CT scan table with the legs fully extended, a coronal image of the whole lower limbs from little above the iliac crests to the heel was taken. With the subject in the same position, the three main joint of the right leg were scanned in the transverse plane. Images of the hip joint (from approximately 50 mm above the acetabulum to 20 mm under the great trochanter) and ankle joint (from roughly 30

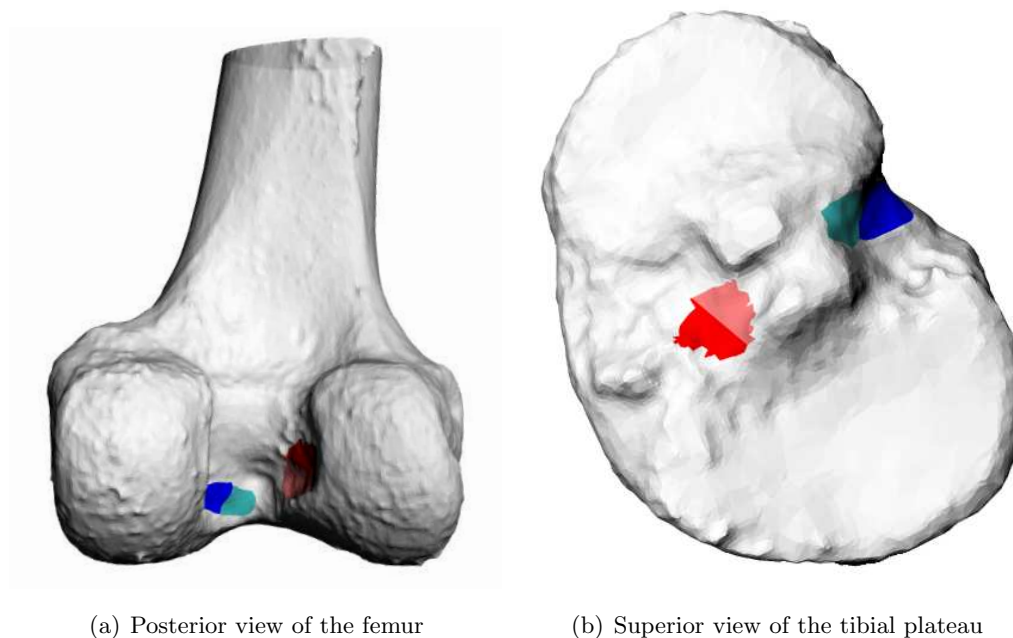


Figure 4.2: Insertion areas of cruciate ligaments: am-ACL (red), pl-ACL (soft red), pm-PCL (blue), al-PCL (soft blue).

mm above the talar mortise to 44 mm under) were acquired with a slice thickness of 5 mm. The knee joint was scanned from 110 mm above the tibial plateau to 94 mm under with a slice thickness of 2 mm. All the images were captured in a 220 mm \times 220 mm field of view and a resolution of 512 \times 512 pixels except for the image of the complete lower limbs (1120 \times 500 mm, 1128 \times 512 pixels).

Data related to the soft tissues (i.e. ligaments and cartilaginous surfaces) were acquired by means of MRI (GE Medical Systems, Signa HDxt). Sagittal and coronal images of the knee joint were captured with the subject placed on table of the MRI in the above mentioned position. Images field of view and resolution were equal to that of the CT scan, image window spans the joint from almost 130 mm above the tibial plateau to about 20 mm under the tibial tuberosity with a slice thickness of 0.8 mm.

The images were processed in order to construct the three-dimensional models of the subject-specific bone surfaces via a segmentation process carried out using dedicated software packages. Those models are fundamental for the investigation allowing for the subject specific data to be stored as a point cloud. The surfaces of the distal femur, proximal tibia and patella were obtained using a temporary license of the Mimics

4. FROM IN VIVO CLINICAL DATA TO THE SUBJECT SPECIFIC MODEL

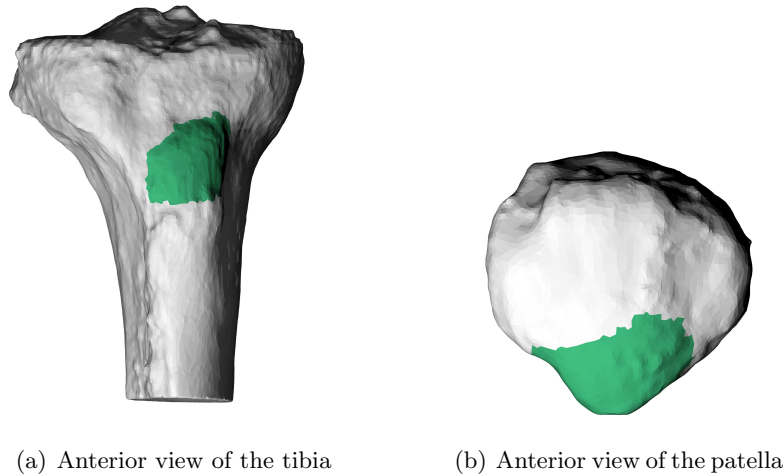


Figure 4.3: Insertion areas of patellar ligament (green) on the tibia and the patella.

Research software (Materialise, Belgium); differently, both the surfaces of the other bone segments and the origin and insertion of the ligaments were reconstructed using the free open source software application ITK-SNAP [50].

As far as the CT images are concerned, the segmentation was initially performed with the automatic tools supplied by the softwares (3D region-growing method) in order to get a first approximation of the surfaces (provided the good contrast of the bone tissue with respect to the surrounding one in the CT images), this first attempt was then perfected by a manual segmentation. The three-dimensional models reconstructed from CT data were used to retrieve the experimental passive motion (as described in the following section) as well as to identify both the bony landmarks of ligaments insertions sites and those useful to define the anatomical frames via virtual palpation. For this reason, besides the proximal tibia and distal femur, also the three-dimensional models of the medial and lateral malleolus and femoral head were reconstructed, allowing for the definition of the anatomical frames of femur (S_{Fa}) tibia (S_{Ta}) and patella (S_{Pa}).

The segmentation process on the MRI images was performed in similar way. The proximal tibia, distal femur and the patella were reconstructed complete with their cartilaginous surfaces as shown in Figure 4.5 where the 3D bone models from the CT scan and the MRI are superimposed.

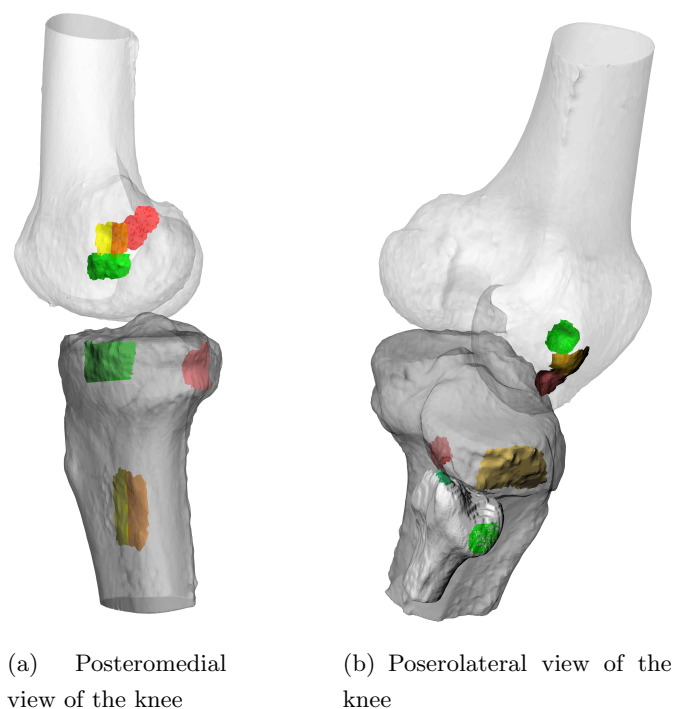


Figure 4.4: Insertion areas of posteromedial and posterolateral structures. On the posteromedial corner: ab-MCL (yellow), pb-MCL (orange), dMCL (soft green), POL (red). On the posterolateral corner: LCL (green), PT (brown), MLCL (yellow), PFL (turquoise) (the insertion areas of PFL on the femur are not shown since are shared with the PT).

4.1.1.2 Ligaments' insertion areas

Ligaments were segmented manually, particular care was taken into the identification of the origin and insertion areas. Different planes were used during ligament's segmentation according to their orientation with respect to the three standard anatomical planes; data from literature concerning dimension and position of the origin and insertion areas with respect to anatomical landmarks were used together with the imaging data for those ligaments whose areas proved difficult to evaluate. The ACL (Fig. 4.2) was mainly segmented using the coronal plane since it appeared too skewed in the sagittal one. On the contrary the PCL (Fig. 4.2) resulted well depicted in this plane making it the most suitable for its segmentation. Attempts were made to discern the double bundle anatomy of the ACL and PCL from MRI interpolating the images on oblique planes (see section 2.2), although the bundles were seldom visible so that a clear identification of those structure in proximity of the attachment areas proved dif-

4. FROM IN VIVO CLINICAL DATA TO THE SUBJECT SPECIFIC MODEL

difficult. As a consequence, their morphology was obtained from literature [15, 21]. The sMCL (Fig. 4.4 (a)) proved difficult to segment both in the sagittal and the coronal plane due to its flat and broad shape, furthermore the images acquired by the MRI end under the tibial tuberosity not enough to allow for a correct acquisition of the images resulting in a darkened area in the region of the sMCL insertion site. For these reasons the segmentation of the sMCL origin and insertion areas were identified both from segmentation and from anatomical and morphological data from literature [23, 27, 45]. Patellar ligament is clearly visible in the sagittal plane, thus this plane was chose for its segmentation, its insertion areas are shown in Figure 4.3. The detection of LCL insertion (Fig. 4.4 (b)) on the fibula was guided by data from literature [8] since its identification proved difficult; its origin on the femur was identified near the lateral epicondyle, however, like the medial collateral ligament, it was difficult to estimate its shape and dimensions so they were taken from literature as well [8]. The structures of the posterolateral and posteromedial corner of the knee were mainly obtained with the aid of remarkable anatomical landmarks associated to their position. This procedure was followed to determine the attachment areas of the POL (Fig. 4.4 (a))[12, 37, 45] and of the MLCL (Fig. 4.4 (b))[24]. Differently, the PT and the PFL were partially visible in coronal planes, their attachment (Fig. 4.4 (b)) were obtained combining the segmentation with literature data [8, 16, 25].

The 3D shape of the ligaments obtained from the MRI was processed in a 3D modelling software (Rhinoceros, Robert McNeel & Associates, Seattle, Washington) and their origin and insertion areas were transformed in a cloud of points on the MRI bone models surface.

4.1.1.3 Anatomical reference frames

Since the models created through segmentation are expressed in native global frames related to the MRI and the CT, a common reference system is needed. In order to have a congruent data set, every point describing an anatomical structure (i.e. attachment areas and articular surfaces) was then represented in the anatomical frame of the bone it belongs to (i.e. S_{Fa} , S_{Ta} or S_{Pa}). As previously stated, the anatomical frames were identified on the CT since the quality of the 3D models obtained allowed for a better estimation of the anatomical landmarks needed to define the frames, so the transformation between the MRI native reference system and the anatomical frames is

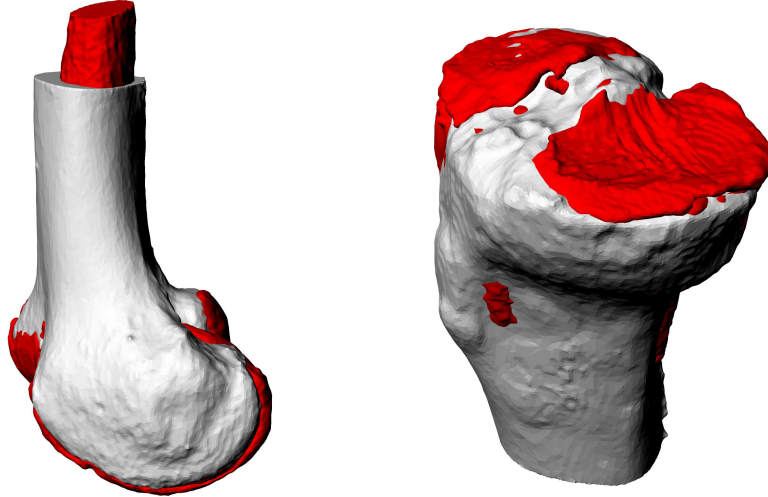


Figure 4.5: Registration of the MRI based models of femur and tibia on the CT based ones. The images show the 3-D models placed in their own anatomical frames.

needed. The affine transformation between each MRI native reference system and the corresponding anatomical frame was found superimposing a set of common anatomical landmarks identified in the MRI model and in the CT model (in its proper anatomical frame). The identification of the anatomical landmarks was carried out manually via virtual palpation using a modelling software (Rhinoceros, Robert McNeel & Associates, Seattle, Washington). The medial and the lateral epicondyles and the most anterior point of the condyles were used as anatomical landmarks for the superposition of the femurs, the intercondylar eminences and the superior edge of the tibial tuberosity were used as anatomical landmarks for the tibia. On the same software the superposition of the MRI models on the anatomical oriented CT models was done using an automatic 3 point orientation function available in the program. The affine transformation between the 3D MRI model in its native reference system and the re-oriented one was done through a MATLAB based algorithm specifically written for the purpose. In Figure 4.5 the result of the superposition of the MRI and CT based models is shown.

4.1.2 Experimental passive motion

The experimental in vivo measurement of passive motion (i.e. the joint motion in virtually unloaded condition) is not a straightforward goal to achieve. Not only a suitable

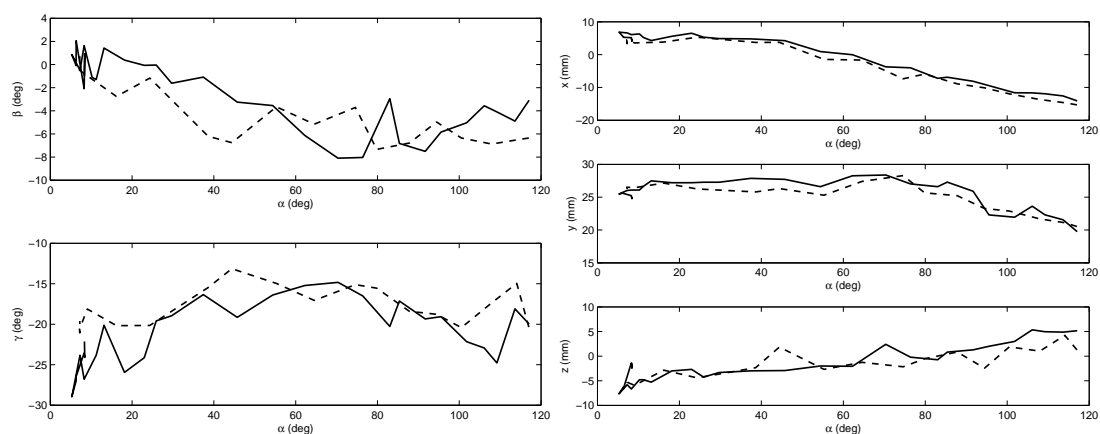
4. FROM IN VIVO CLINICAL DATA TO THE SUBJECT SPECIFIC MODEL

TF joint	α (deg)	β (deg)	γ (deg)	x (mm)	y (mm)	z (mm)
mean \pm SD		2.06 ± 1.37	2.02 ± 1.86	1.20 ± 0.74	1.08 ± 0.52	1.76 ± 1.55
max		4.75	7.73	3.31	2.04	4.81
PF joint	α (deg)	β (deg)	γ (deg)	x (mm)	y (mm)	z (mm)
mean \pm SD	2.30 ± 1.37	4.47 ± 3.45	4.30 ± 3.09	1.33 ± 0.89	1.37 ± 0.68	1.30 ± 1.14
max	4.17	12.94	9.84	3.62	2.87	5.80

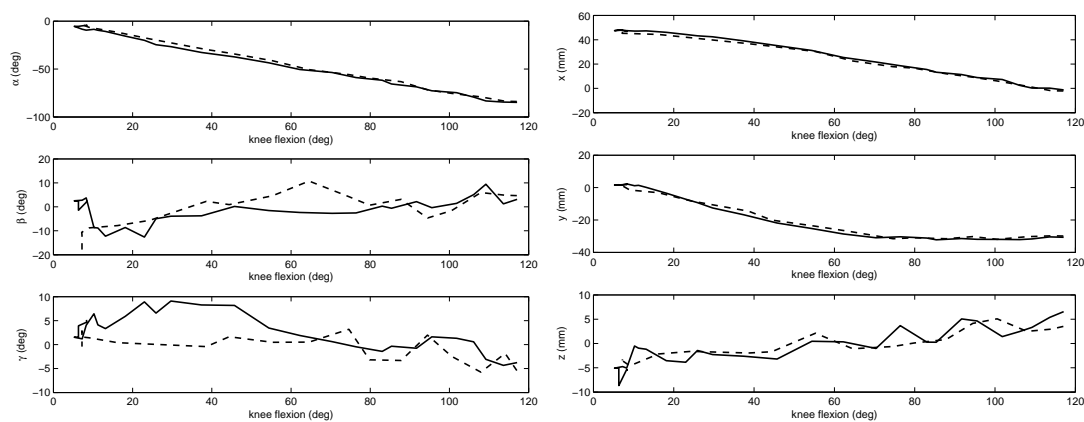
Table 4.1: Statistical analysis of the data: mean value, standard deviation (SD) and maximal difference in the acquired motion between flexion and extension movement.

measurement of the bones relative motion but also a correct reproduction of it are two crucial aspect to deal with. The experimental passive motion was recorded through a single-plane fluoroscopy (CAT Medical Systems, Hiris Rf43) of the knee joint flexion in the sagittal plane. The subject was placed on the fluoroscope supine with a wedge-shaped cushion behind his back in order to ensure that the muscles of the lower limb were not tight and avoid muscular contraction during the test. The right heel was put on a polytetrafluoroethylene disc so that it could slide with low friction on a straight glide situated under the shank, a lace was tied around the thigh to allow the subject to pull his leg toward his chest. After an initial set up, the subject was asked to flex the lower limb slowly (in order to reduce the inertia forces acting on the lower limb) by pulling the lace until the complete flexion of the knee and then to push it back in the full extended position. Provided that the dimension of the detector screen did not allow for the whole range of flexion to be completely recorded in only one take, the movement has to be split into two trials. In both trials the subject performed a complete flexion-extension cycle but the position of the subject with respect to the X-ray source and detector of the fluoroscope was changed so that the first trial acquired the experimental passive motion over a flexion arc from 0 to almost 95 degrees and the second trial acquired the motion in a range from 85 to 130 degrees. Acquiring the motion in two different trials is thought not to affect the investigation given that a relative motion is studied and the difference between the two takes are supposed little and due to hysteresis. Both the trials lasted about 4 seconds and the experimental passive motion was recorded at 15 fps.

The frames acquired through the fluoroscope show the projection on the sagittal plane of experimental passive motion of the knee (Fig. 4.7). In order to retrieve the



(a) Rotational components of the TF joint motion. (b) Translational components of the TF joint motion.



(c) Rotational components of the PF joint motion. (d) Translational components of the PF joint motion.

Figure 4.6: The experimental passive motion acquired through single-plane fluoroscopy. All the components of the motion are represented against the knee flexion angle. The solid line is the movement in the flexion arc the dashed one is the movement during the extension.

4. FROM IN VIVO CLINICAL DATA TO THE SUBJECT SPECIFIC MODEL

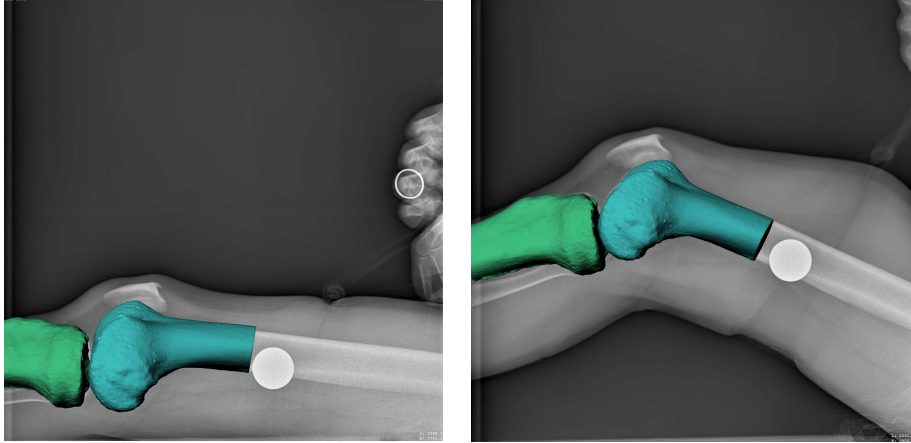


Figure 4.7: The matching of two frames of the fluoroscopy in the case of the tibio-femoral joint. The fluoroscopic projection plane is shown with the superposition of the 3-D models of tibia and femur (the images are a representation of the procedure and are not related to the software adopted in the study).

spatial motion, a matching between the three-dimensional bone models and the projection of the bones on the aforementioned plane is sought for every frame of the images sequence (Fig. 4.7). The matching process (called registration) of the 3-D models onto the 2-D projection plane was carried out using the Kneetrack software [3]. The pose of each bone was found by manually superimposing the contour of the 3-D models on every image. The bone models are superimposed to the fluoroscopic projection plane which is provided with a global reference system as well as each bone model is provided with a local one. Controlling the six parameters that define the pose of the bone with respect to the projection plane (i.e. the translations along the global reference system axes and the rotations around the axes of the bone's local system), it is possible to determine the best match between the planar contour of the three-dimensional model and the projection of the bones on the plane. As a consequence, the spatial pose of each bone is obtained per each frame of the images sequence of the fluoroscopy allowing for the determination of the spatial motion of the knee joint. The relative motion of the TF and PF joints is expressed by means of the Grood & Suntay convention (as explained in section 2.3).

In Fig. 4.6 the experimental motion acquired through the single-plane fluoroscopy is shown. Differences in the quality of the acquired data are visible between the motion

components that lies in the plane of the fluoroscopy and those that lie outside. The first one (namely the anterior/posterior and superior/inferior translations in both the sub-joints and the patellar flexion in the PF sub-joint) appear more regular and smooth, a greater agreement is noticeable between the flexion and the extension; the second one, on the contrary, show marked differences between the two movements and higher irregularity. Table 4.1 confirms the dissimilar quality of the acquired data. Observing the differences between the value of a motion component during flexion and extension movement, it is easy to see that, in almost every case, the components that lie outside the fluoroscopy plane show higher values of the maximum difference, higher mean value and higher standard deviation. The differences between the patterns of the two motions are related to hysteresis and to alignment imprecision in the matching of motion components outside the fluoroscopy plane. Although, the first one are usually small (as it is possible to notice in the motion components in the fluoroscopy plane) so that the major contribution is due to motion artefacts related to the single-plane fluoroscopy. The most critical motion components to match revealed to be the rotations, in particular the components β and γ of the PF joint. The higher uncertainties linked to this components of the patello-femoral motion are due to the high symmetry of the patella, the use of single-plane fluoroscopy makes difficult to get a precise match of highly symmetrical objects.

4.1.3 Clinical tests on the laxity of the knee

Since the experimental sessions were conceived and focused specifically on the kinematic of the knee joint, no clinical tests on the subject were carried out to obtain data to define the stiffness model of the joint. Therefore, the model was based on a reference paper [13] whose experimental set-up has been reproduced in numerical simulations and its data used in the identification procedure. This paper was chosen for the detailed account of the experimental procedure followed, regarding in particular the precise description of the constraints and the loading conditions applied to the knee.

The reference paper reports clinical tests produced on intact specimens in order to evaluate the limits of movement of the human knee in different loading conditions. The test are performed in vitro by means of a test rig on nine lower limbs. The limbs are mounted on the rig so that the femur is clamped to a moving platform whose motion provides the different flexion angles, the tibia is allowed to hang without constraints

4. FROM IN VIVO CLINICAL DATA TO THE SUBJECT SPECIFIC MODEL

under its own weight. Different loading conditions are applied to the tibia according to the clinical tests reproduced, all the tests are performed at different flexion angles from full extension to 90 degrees of flexion with increments of 15 degrees each step. An instrumented linkage is used to measure the motion of the tibia under the different loading conditions.

The clinical test performed in the paper are:

- *Anterior/Posterior drawer*: a 100 N force directed anteriorly (or posteriorly) with respect to the tibia is applied to the shank 25 mm distal to the knee joint line. Its displacement with respect to a reference pose is obtained. At every flexion angle the pose of the tibia under the effect of its own weight is considered as the reference position.
- *Abduction/Adduction test*: a varus/valgus moment of 20 Nm is applied to the tibia and its adduction (or abduction) with respect to the femur retrieved. The angular displacement of the tibia with respect to a reference pose is obtained. The fully extended position is used as the zero-rotation reference.
- *Internal/External rotation test*: an internal (or external) moment of 5 Nm is applied to the tibia, its rotation with respect to a reference pose is obtained. The reference pose is the same adopted for the ab/adduction test

In addition to the loading condition related to each clinical test, a small counterforce is applied to the foot in order to fix the flexion angle.

It is worth noting that in the reference paper only the most clinically relevant displacements are reported for every loading condition, even though the complete pose of the specimen was assessed during the experiment. For this reason, in the following, only one parameter of motion per test is considered although in both the reference paper and the present study the tibia is free to move without constraints (except for the imposed flexion angle).

4.2 The identification of the subject specific model

4.2.1 First guess of the parameters

In order to define the subject specific model, a first guess of the models' parameters had to be defined. As far as the kinematic model is concerned, a preliminary definition

4.2 The identification of the subject specific model

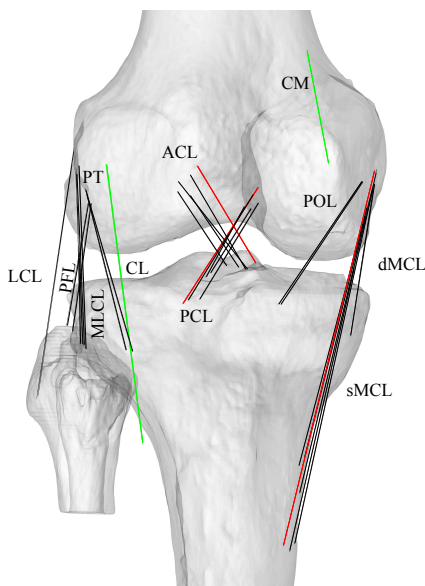


Figure 4.8: The fibres of the stiffness model. The green one are the isometric fibres relative to the articular contacts, the red ones are those related to the ACL, PCL and sMCL

of its geometry comes from the data collected from CT scan, MRI and fluoroscopy (as described in section 4.1). In order to define the TF initial geometry an estimation of the isometric fibre had to be found from the point cloud of the origin and insertion areas of ligaments (ACL, PCL and sMCL). This fibre is determined choosing the couple of points (one belonging to the origin on the femur, the other to insertion on the tibia) that exhibits the minimal variation of distance during the whole range of the experimental passive motion. Since the experimental motion obtained from the fluoroscopy is affected by some uncertainties, the research of the isometric fibres of ACL, PCL and sMCL ligaments is limited to the bundle where they are experimentally located [4]. Accordingly, only the antero-medial bundle of the ACL, the postero-medial bundle of the PCL and the anterior bundle of the MCL were considered. Once the isometric fibre of each ligament is identified, its endpoints locate the centres of the spherical pairs \mathbf{c}_{ti} and \mathbf{c}_{fi} ($i = 1 \dots 3$) that constitute three links out of five of the 5-5 parallel mechanism. The centres of the other two rigid links (\mathbf{c}_{tj} and \mathbf{c}_{fj} , ($j = 4, 5$)) relative to the articular surfaces come from the centres of best fitting spheres to the medial and lateral condyles of the femur and the tibia. This spheres were determined by means of the Rhinoceros software sphere fitting algorithm from point clouds extracted from the MRI models.

4. FROM IN VIVO CLINICAL DATA TO THE SUBJECT SPECIFIC MODEL

The lengths l_i are the distances between the origin and insertion of each isometric fibre at the reference position (i.e. full extension).

Regarding the PF joint, the isometric fibre of the patellar ligament is determined with the same procedure adopted for the ligaments of the TF joint. The relative pose of the patella with respect to the femur at an angle in the midway between the full extension and the full flexion is chosen as the reference pose for the PF joint. The axis \mathbf{n}_p was determined as the axis connecting the centres of the best fitting spheres to the anterior part of the femoral condyles, an arbitrary point \mathbf{q}_p is chosen on this axis; the axis \mathbf{n}_f and the point \mathbf{q}_f are obtained projecting \mathbf{n}_p and \mathbf{q}_p in S_{Fa} . The initial estimation of the parameter λ_0 is obtained computing the distance between \mathbf{q}_p and \mathbf{q}_f in the reference pose while λ_1 comes from the angle between \mathbf{n}_p and the normal to the plane containing the intercondilar space.

As far as the stiffness model is concerned (Fig. 4.8), the crucial point is the determination of the fibres to include in the model, that is to say how to select the fibres from the cloud of points of the origin and insertion areas. Great attention was given to the identification of anatomically oriented fibres [32]. As a guidance to the choice of suitable fibres to represent the bundles of the ligaments, a map of the deformation of the fibres of each ligament was obtained computing for each point of the less dense insertion area the ratio between the maximum elongation and the maximum length of the most isometric fibre obtainable from that point. The motion obtained from

Ligament bundle	Number of fibres
<i>am-ACL</i>	2 plus 1 isometric fibre
<i>pl-ACL</i>	2
<i>pm-PCL</i>	2 plus 1 isometric fibre
<i>al-PCL</i>	2
<i>sMCL</i>	5 plus 1 isometric fibre
<i>dMCL</i>	2
<i>LCL</i>	3
<i>MLCL</i>	4
<i>PT</i>	2
<i>POL</i>	2
<i>PFL</i>	2

Table 4.2: Ligament bundles and number of fibres per bundle considered in the stiffness model.

the kinematic model was used to compute the map of the deformation of the fibres of the ligaments. A number of fibres within those that showed the lowest deformation were chosen provided that their orientation was anatomically coherent. ACL, PCL and sMCL ligaments comprise the isometric fibres defined in the previous step of the sequential procedure, the parameters of the articular contacts of medial and lateral condyles of femur and tibia come from the kinematic model as well. In Table 4.2 the ligaments considered in the model are reported together with the number of fibres used to model each bundle. The number of fibres per ligament adopted in the present study were chosen in accordance with [30].

The initial estimate of stiffness values are derived from literature [6, 22, 30, 36] while the first guess of the unloaded length of the ligaments is defined and explained in section 3.2.

4.2.2 Optimization of the models parameters

4.2.2.1 Kinematic model

In order to define a precise model of the joint behaviour, a refinement of the first estimate of the parameters is needed. The research of the optimal set of parameters is done by means of an optimization procedure. The optimization is performed separately on the kinematic model first and then on the stiffness model in accordance with the sequential approach.

The optimization process on the kinematic model is performed in two consequential steps: the model of the TF sub-joint at first and then the PF one. The procedure can be summarized in the following steps (given that the process is conceptually the same, in the following no distinction are made between the TF and the PF sub-chains):

1. A first estimate x_0 of the parameters defining the geometry of the model is given as starting point for the first iteration of the optimization procedure. Together with it, the set of boundaries and constraints that define the search domain of the parameters is defined;
2. The closure equations are solved for the mechanism whose geometry is defined by x_0 and its pose computed for every flexion angle considered. The closure equations (3.1) and (3.2) of the TF and PF sub-chains respectively, are solved with the function *fsolve* (MATLAB);

4. FROM IN VIVO CLINICAL DATA TO THE SUBJECT SPECIFIC MODEL

3. If the closure of the mechanism is satisfied at every flexion angle, the motion obtained by the mechanism is compared with the experimental one. In order to estimate the fitting between the two, an objective function is defined as:

$$F = \sum_{i=1}^{n_p} \sum_{j=1}^{n_\alpha} \epsilon_{ij} \quad (4.1)$$

where the first summation is on the number of unknowns n_p and the second is on the number of pose (i.e. flexion angles) considered n_α . The term ϵ_{ij} is defined as:

$$\epsilon_{ij} = \frac{(x_{ij} - \tilde{x}_{ij})^2}{\Delta \tilde{x}_i^2} \quad (4.2)$$

where x_{ij} is the value of the unknown x_i (i.e. the components of the TF and PF joints motion) in the j -th pose, \tilde{x}_{ij} the experimental value of the same unknown in the same pose and $\Delta \tilde{x}_i$ is the difference between the maximum and the minimum value of the i -th unknown observed experimentally. The term ϵ_{ij} is thought as an estimate of the discrepancy between the calculated value and the experimental one with respect to the range of variation of the parameter. If the closure equation is not satisfied, an arbitrary high value is assigned to F meaning that the set of parameters is to be rejected;

4. The optimization algorithm corrects the values of the parameters according to the result of the evaluation of F , a new set of corrected parameters is given for the following iteration;
5. The procedure iterate until it reaches a minimum of the objective function; if a minimum is reached or user defined stop criteria are satisfied, the process ends.

Each optimization process is carried out in two subsequent steps: in the first one a *genetic algorithm* (MATLAB, The MathWorks Inc.) was used in order to obtain a first evaluation of the region in the domain of the parameters where a reliable global optimum could be; in the second one the solution of the genetic algorithm is given as input for the *fmincon* algorithm in order to refine it. The combination of genetic algorithm and *fmincon* was necessary, since the high non-linearity of the objective function as well as the discontinuities introduced in case of non resolution of the closure equations proved difficult to handle directly with a derivative-based algorithm.

4.2 The identification of the subject specific model

It is important for the purpose of the optimization to understand the limits of the search domain of each parameter. This is a crucial aspect indeed, larger search domains allows for a precise fitting of the model to the experimental data but at the price of missing anatomical relevance and subject specificity. On the contrary, too strict boundary limits make the optimization process meaningless. Thus a good balance between the two tendencies has to be found considering the uncertainties that affect the preliminary estimates of the parameters as well as at the purpose of the study. To enhance the subject specific character of the study as well as the predictive possibilities of the models, the search domains of each parameter was kept as narrow as possible.

The coordinates of the origin and insertion points of the isometric fibres of ACL, PCL, MCL were kept within a sphere of radius $r_l = 2$ mm centred in the first estimate, in the case of the PL the radius was equal to 4 mm due to the worst quality of the grid of points. The optimal length of the isometric fibres was allowed to vary within a range of values included in $l_{init} \pm r_l + \epsilon$ (l_{init} is the initial values of the length of the fibres, namely their length in the reference position). The value ϵ , assumed equal to $l_{init}/100$, is to take into account a little tightness of the fibres of the ligaments at full extension. A larger bound, a spherical domain of radius $r_c = 5$ mm around the first estimate, was kept for the points defining the articular contact given that a precise segmentation of cartilaginous surfaces of the femur and the tibia at their contact region proved difficult to be done due to the difficulties to find a clear demarcation between the two surfaces.

	<i>First guess</i>			<i>Identified parameters</i>		
\mathbf{n}_f (mm)	0.1529	0.5282		0.1279	0.2709	
\mathbf{Q}_f (mm)	10.2207	2.3771		10.2384	3.8349	
\mathbf{n}_p (mm)	0.2188	1.2545		0.1994	1.0657	
\mathbf{Q}_p (mm)	-34.2275	5.6835		-34.9423	4.4126	
PL Tibial attachment (mm)	36.6405	-48.3130	-14.6816	33.9638	-47.3085	-11.8841
PL Patellar attachment (mm)	13.1597	-7.7843	-0.4268	16.4925	-9.4305	-1.9040
Fibre length (mm)	80.6362			78.2451		
λ_0 (rad)	0			-1.9306		
λ_1 (rad)	2.1333			-1.1788		

Table 4.3: The results of the identification process on the patello-femoral sub-chain.

Femur attachments	ACL (mm)			PCL (mm)			sMCL (mm)			LC (mm)			MC (mm)		
<i>First guess</i>	-8.2579	-3.1408	7.2818	-3.5987	-10.2109	-6.5335	-6.8998	-5.2733	-40.0801	-0.4450	-1.1199	29.3156	-1.8282	-1.5579	-21.9842
<i>Identified parameters</i>	-7.4309	-2.3550	7.0017	-2.5538	-8.8149	-7.5124	-6.2697	-4.5883	-39.4240	1.3828	-2.7579	33.3183	-3.0813	-2.6212	-26.7056
Tibia attachments	ACL (mm)			PCL (mm)			sMCL (mm)			LC (mm)			MC (mm)		
<i>First guess</i>	9.0531	-2.9585	-12.4037	-11.7576	-12.9486	12.6787	9.0221	-75.1279	-20.9511	13.5679	-47.6731	17.3981	-17.1112	52.4767	-23.4767
<i>Identified parameters</i>	10.4620	-1.5530	-12.2792	-10.7204	-11.6959	12.0578	10.3575	-74.2137	-19.7791	13.1536	-48.1282	16.8076	-13.8250	53.6986	-19.9130
Fibre lengths	ACL (mm)			PCL (mm)			sMCL (mm)			LC (mm)			MC (mm)		
<i>First guess</i>	30.4275			39.4004			100.2719			72.5255			31.0999		
<i>Identified parameters</i>	30.4349			40.4525			101.2193			73.0729			31.3099		

Table 4.4: The results of the identification process on the tibio-femoral sub-chain. The table shows a comparison between the initial guess of the parameters and the identified ones. LC stands for lateral contact fibre while MC stands for the medial one.

4.2 The identification of the subject specific model

As far as patello-femoral sub-chain is concerned, the optimal longitudinal axis of the cylinder defining the articular contact between the femur and the patella was constrained both in the maximal distance (2 mm) and in the maximal inclination (2.5 degrees) with respect its first estimate.

4.2.2.2 Stiffness model

The optimization process of the stiffness model is similar to the process described in the previous section for the kinematic one:

1. A first estimate of the parameters is given as input together with the lower and upper boundaries of the search domain of the parameters;
2. The equilibrium position of the tibia is computed for 6 different loading conditions (i.e. 2 loading conditions for each clinical test considered, according to the reference paper) every 15 degrees of flexion angle from full extension to 90 degrees of flexion. The nonlinear equation solver *fsolve* (MATLAB) is used to determine the equilibrium pose solving the Eq. (3.9). In order to enhance the stability of the algorithm the flexion arc was subdivided in ninety steps so that the equilibrium pose was computed at every flexion angle from 0 to 90 degrees. At each flexion angle the starting point for the solver is provided by the solution at the previous one. The starting point vector is composed of the 5 parameters that define the pose of the tibia with respect to the femur (the flexion angle α is imposed) plus the magnitude of the constraint couple needed to fix the flexion angle;
3. If the equilibrium is satisfied for every clinical test at every flexion angle, the displacements obtained solving the equilibrium equations for the tibia under the different loading conditions are compared to the displacement reported in the reference paper (see section 4.1.3). In order to refer the displacements, a reference position is set for every test (as explained in section 4.1.3). A function is defined to estimate the gap between the displacements obtained and those of the reference paper:

$$F = \sum_{i=1}^{n_t} \sum_{j=1}^{n_\alpha} \frac{\left(\delta_{ij}^+ - \tilde{\delta}_{ij}^+\right)^2 + \left(\delta_{ij}^- - \tilde{\delta}_{ij}^-\right)^2}{2\Delta\tilde{\delta}_{ij}^2} \quad (4.3)$$

4. FROM IN VIVO CLINICAL DATA TO THE SUBJECT SPECIFIC MODEL

where the two summations are on the clinical tests performed (i.e. the anterior/posterior drawer, the ab/adduction and the internal/external rotation tests) and on the considered flexion angles respectively; n_t is the total number of clinical tests and n_α is the total number of flexion angles. The symbol $\tilde{\delta}$ is the displacement reported in the reference paper while δ is the calculated one with respect of a reference position, $\Delta\tilde{\delta}_{ij} = \tilde{\delta}_{ij}^+ - \tilde{\delta}_{ij}^-$. The apices + and - indicate the two different directions of application of the loads in each of the clinical test considered;

4. If the equilibrium is not satisfied or every loading condition on the whole flexion arc, the function F is given an arbitrary high value to indicate a set of parameters to be discarded. The Eq. (4.3) is the objective function to be minimized in order to identify the optimal set of parameters that constitute the stiffness model of the knee. Similarly to the optimization of the kinematic model, the optimization process is carried out by means of a genetic algorithm since it proved more efficient than a quasi-Newton method even though more time consuming.

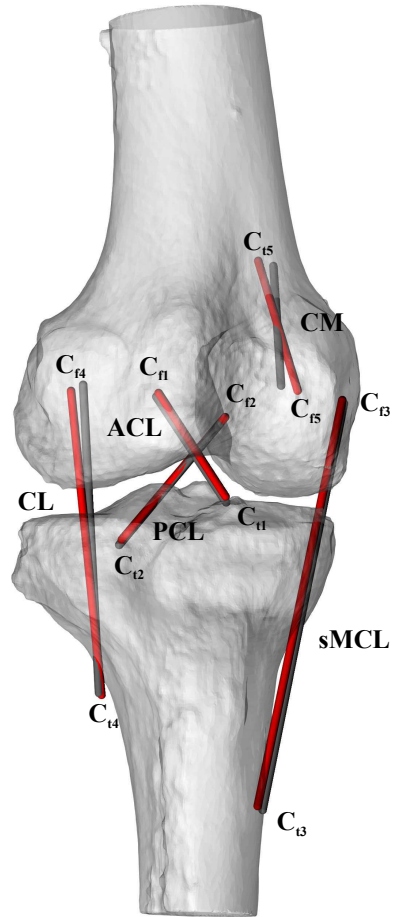
The definition of the upper and lower bounds for the parameters of the stiffness model, that is to say the zero-load length l_{i0} of the fibres and their stiffness k_i , is a critical and fundamental aspect of the model. While the stiffness is allowed to vary within a range of values based on the literature, the boundary of the initial lengths has to be decided considering that the stiffness model is deeply linked with the kinematic one. As a consequence, every structure added to model the stiffness of the joint as well as every variation of l_{i0} with respect to the value obtained from the kinematic model should not interfere with the passive motion. Some preliminary investigations were done on the zero-load lengths of the ligaments with the purpose to determine their lower bound. These investigations were thought also to furnish some hints on the amount of reduction allowed to the lengths l_{i0} of the ligaments and to the length of the isometric fibres. In fact the last ones work on a limit configuration between being tight or slack and the possibility of a little physiological tightness of the isometric fibres is not to be discarded. These preliminary studies consisted of a first optimization of the zero-load lengths and of the stiffness of the ligaments trying to fit the passive motion obtained from the kinematic model with the motion of the joint under the action of the weight of the shank and the foot. Indeed, provided the low magnitude of the force due

Ligament bundle	k (kN)										l_{i0} (mm)													
	<i>First guess</i>					<i>Identified parameters</i>					<i>First guess</i>				<i>Identified parameters</i>									
am-ACL	6.59	6.80	7.96			6.80	6.36	7.81			28.91	30.97	30.43			27.54	29.42	28.91						
pl-ACL	5.64	5.33				5.81	4.37				23.46	25.65				22.33	24.77							
pm-PCL	13.67	12.04	12.68			11.72	11.98	13.07			39.32	40.10	40.45			37.35	38.23	38.45						
al-PCL	10.30	10.29				10.25	10.29				33.82	35.23				32.32	34.18							
sMCL	8.37	10.39	10.39	7.70	10.40	9.40	8.42	9.01	8.52	7.31	8.09	9.58	102.32	76.85	79.73	84.98	96.27	101.21	97.42	74.34	76.45	80.74	92.02	96.84
dMCL	1.50	2.08				1.56	2.07				44.19	44.94				42.16	42.69							
LCL	2.10	2.10	2.10			2.06	1.79	2.09			63.99	65.39	65.64			65.03	66.33	66.31						
MLCL	1.00	1.00	1.00	1.00		0.70	1.03	0.98	0.88		45.21	44.9757	46.03	47.80		45.27	45.36	46.77	48.68					
PT	4.79	5.32				4.20	4.80				53.13	52.17				53.50	49.82							
POL	3.17	3.90				3.17	3.57				40.16	40.08				38.18	38.25							
PFL	2.12	2.12				1.84	1.69				43.99	45.96				44.85	46.87							
LC	1000.00					985.04					73.07					74.53								
MC	1000.00					700.00					31.30					29.76								

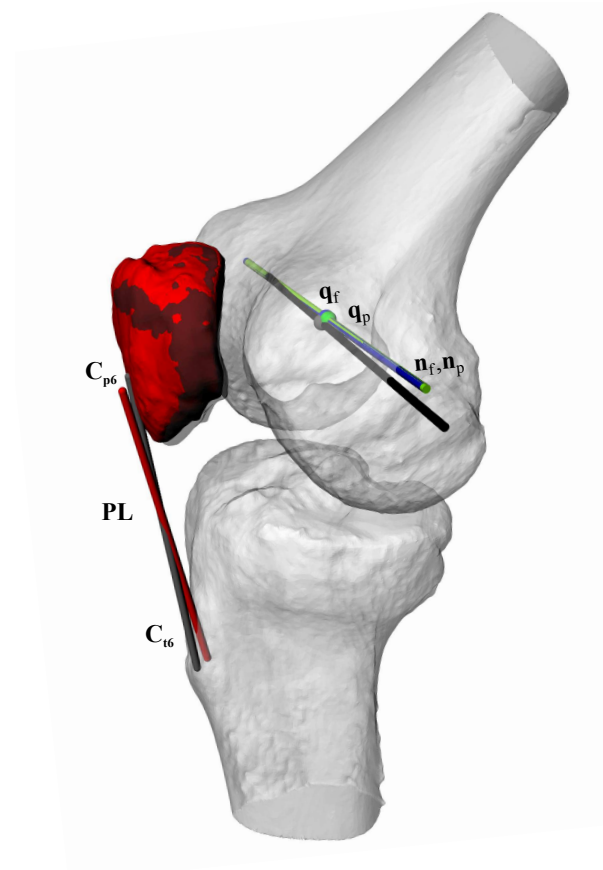
Table 4.5: The results of the optimization on the parameters of the stiffness model. LC and MC stand for the lateral and the medial contact respectively, the bold characters indicate the isometric fibres.

4. FROM IN VIVO CLINICAL DATA TO THE SUBJECT SPECIFIC MODEL

to the weight, the differences between the two motions are expected to be small and the force generated in each ligament moderate. Results of the preliminary investigations showed that a good agreement with the two motion is found with a reduction of the lengths l_{i0} of 5% with respect to the value determined by the kinematic model (see section 3.2). According to these observations, the lower bound for l_{i0} was setted at the 95% of the maximal length obtained during the passive motion of the kinematic model, the upper bound was fixed at its 102% in order to ensure that, in the optimized model, all the fibres contribute to the stiffness of the joint.



(a) Model of the tibio-femoral joint.



(b) Model of the patello-femoral joint. The joint is represented in the reference position.

Figure 4.9: Comparison between the kinematic models of the TF and PF joint before and after the optimization processes.

4. FROM IN VIVO CLINICAL DATA TO THE SUBJECT SPECIFIC MODEL

sub-joint	α (deg)	β (deg)	γ (deg)	x (mm)	y (mm)	z (mm)
TF joint		1.46	2.19	3.32	1.14	1.06
PF joint	6.17	4.14	4.38	1.96	2.53	1.53

Table 4.6: Mean absolute error of the motion components of the TF and PF joints.

4.3 Results and discussions

The kinematic and the stiffness models presented in the dissertation are both based on the part of the experimental motion acquired during the flexion movement.

4.3.1 Kinematic model

The results of the kinematic model are shown in Fig. 4.10 and Fig. 4.11. The position and orientation of the femur with respect to the tibia are shown in Fig. 4.10 (a) and 4.10 (b). The five components of the tibio-femoral motion (i.e. the ab/adduction, internal/external rotations and the three translations) are plotted against the flexion angle, the black dashed line is the experimental motion, the blue line is the motion obtained from the kinematic model of the TF joint. Likewise, the motion of the PF joint is shown in Fig. 4.11 (a) and 4.11 (b) in which the components of the motion of the patella with respect to the femur are plotted against the flexion angle. In the Figure 4.9 the TF sub-chain (Fig. 4.9 (a)) and the PF sub-chain (Fig. 4.9 (b)) are represented, the first guesses of the parameters are represented together with their final value. In the Figure 4.9 (a) the grey bars are the first guesses of the isometric fibres, the red one are the optimized isometric fibres (identically is for PL in Fig. 4.9 (b)). In the Figure 4.9 (b) the black axis is the first guess of \mathbf{n}_p and \mathbf{n}_f ($\mathbf{n}_p \equiv \mathbf{n}_f$) while black sphere is $\mathbf{q}_p \equiv \mathbf{q}_f$, the coloured one (blue and green for the parameters belonging to the femur and the patella respectively) are the same parameters after the optimization. The two patellae in Figure 4.9 (b) are the patella in the experimental pose (the clear one) and in the position obtained bay the model (red one) for the same pose of the TF joint. Tables 4.4 and 4.3 reports the numerical value of the parameters before and after the optimization. The mean absolute error (MAE) for each component of the motion is reported in Table 4.6.

The results show a good agreement between the experimental motion and the one obtained from the kinematic model in the case of the tibio-femoral joint. In particular low discrepancies are noted in almost all the components of the motion, only the anterior translation shows a little higher error than the one shown by the other components.

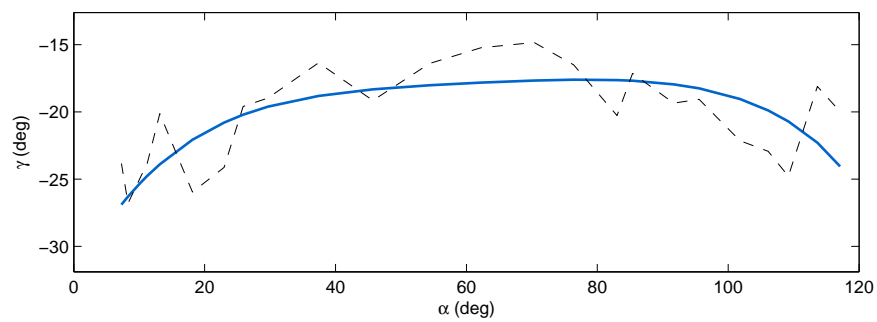
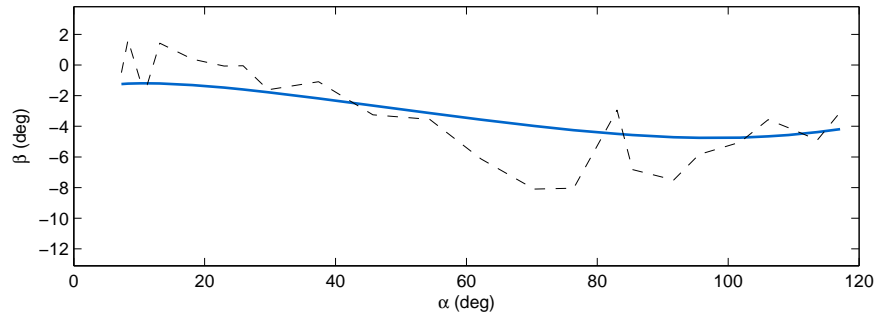
The patello-femoral model seems more critical. In particular, the agreement between the experimental motion and the one obtained by the kinematic model as far as the rotations are concerned is not as good as it is in the case of the TF joint (Table 4.6). However, the experimental motion of the PF joint acquired during the flexion movement and used to obtain the kinematic model of the PF joint appears to be affected by uncertainties in the matching of the pose of the patella. In particular, the component that is likely to be the most affected is the rotation γ (mainly in the first half of the knee flexion arc) which is one of the components whose precise evaluation from single-plane fluoroscopy is most difficult.

The experimental motion acquired during the flexion movement of the subject was chosen to create the PF joint model so as to have a complete coherent model of the joint. Nevertheless, the motion acquired during the extension appears to be more adherent to the physiological one for the PF joint. With regard to this, it is worth noting that the kinematic model of the PF joint created on the motion acquired during the extension of the knee demonstrates higher adherence to the experimental data. Figure 4.12 shows the experimental motion acquired during the extension of the knee and the one obtained by the model. Comparing Fig. 4.11 and Fig. 4.12 it is possible to see the higher adherence between the motion obtained by model and the experimental motion acquired during the extension, in particular a great improvement is noted for the rotation γ whose MAE drops to 1.73 degrees. The mean absolute error for the other components is 4.76 and 4.79 degrees for α and β respectively, 1.80 mm for the anterior/posterior translation (x), 1.30 mm for the inferior/superior translation (y) and 1.18 mm for the medio/lateral translation (z).

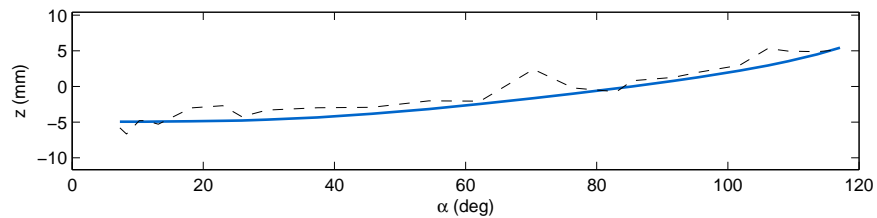
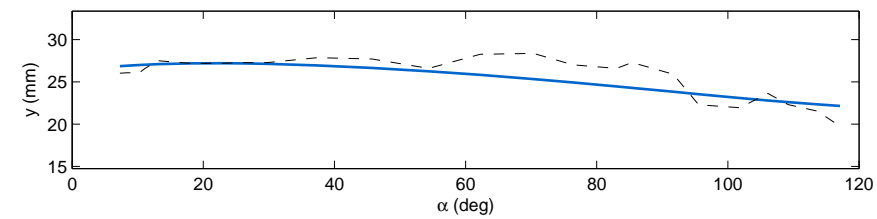
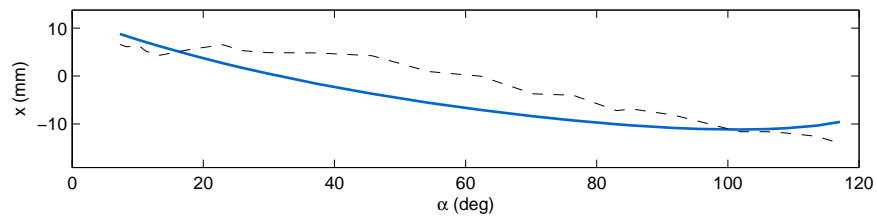
4.3.2 Stiffness model

The results of the stiffness model are shown in Fig. 4.13; the blue line is the displacement obtained from the model, the dashed line is the displacement reported in the reference paper. A good agreement is revealed between the data from the reference paper and the stiffness model in almost all the loading conditions. The mean absolute error observed

4. FROM IN VIVO CLINICAL DATA TO THE SUBJECT SPECIFIC MODEL

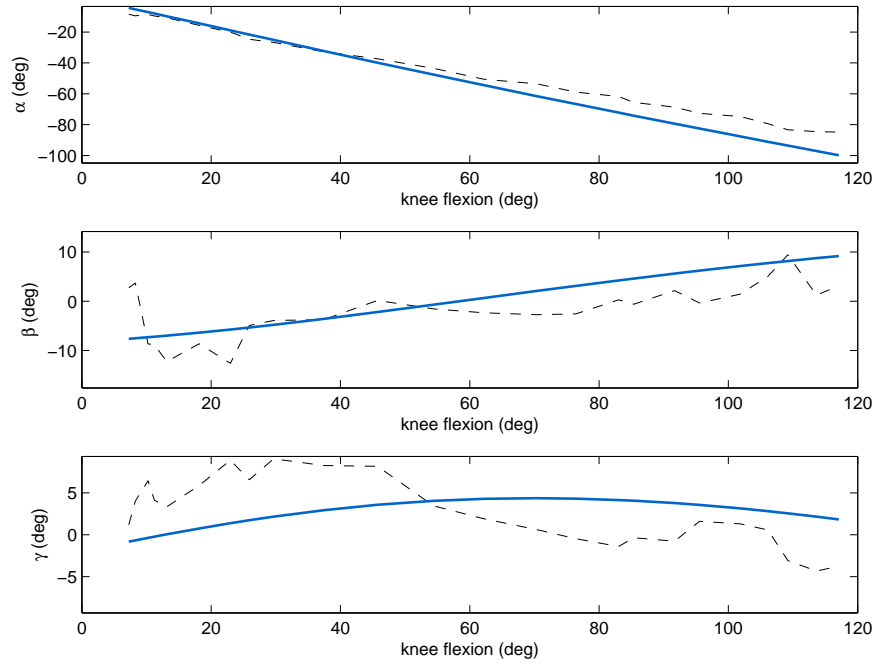


(a) The rotational components of the TF joint motion

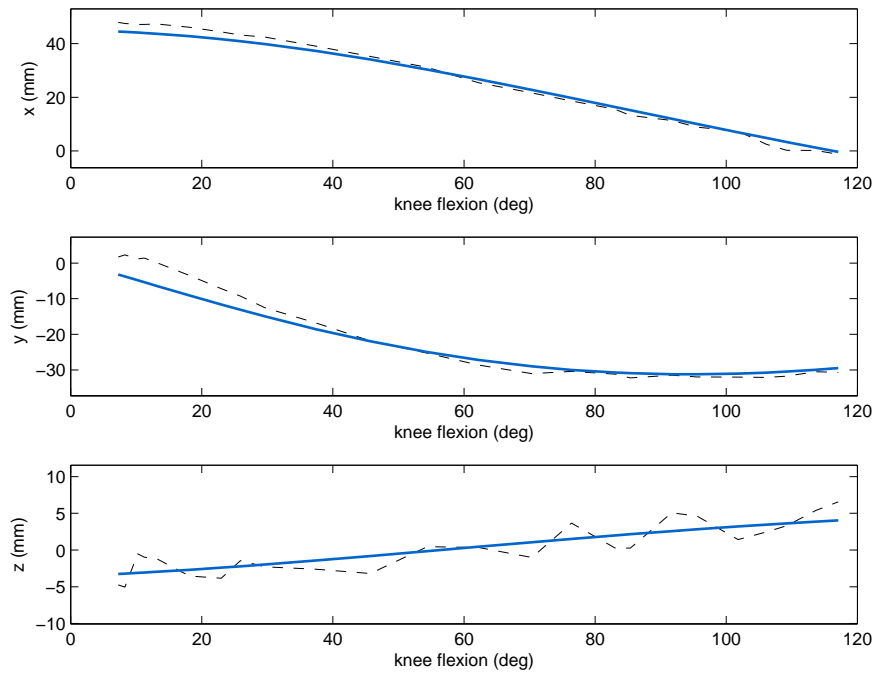


(b) The translational components of the TF joint motion

Figure 4.10: The experimental motion and the calculated one are shown: the black dashed line is the experimental motion, the blue line is the calculated one



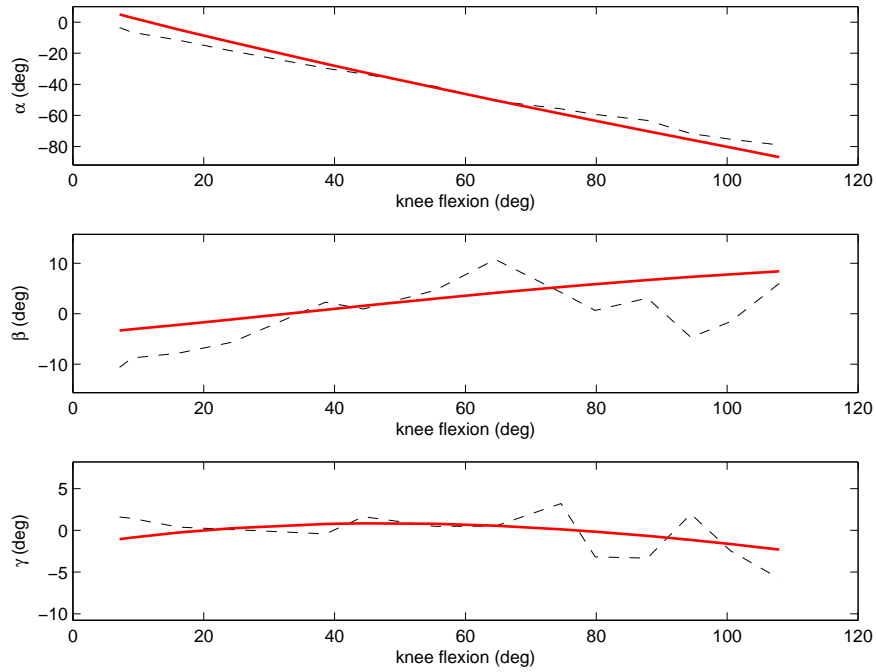
(a) The rotational components of the PF joint motion



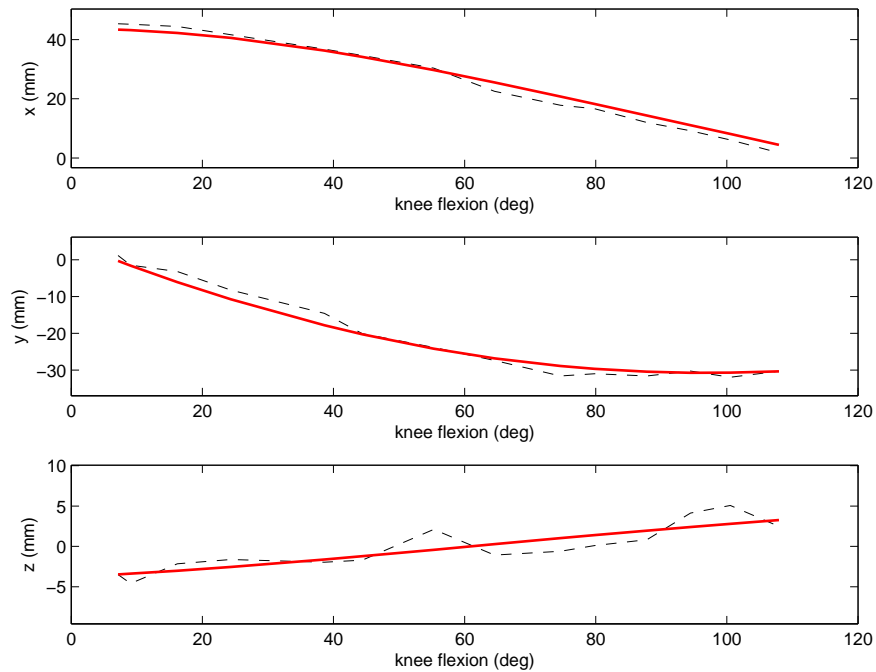
(b) The translational components of the PF joint motion

Figure 4.11: The experimental motion and the calculated one are shown: the black dashed line is the experimental motion, the blue line is the calculated one

4. FROM IN VIVO CLINICAL DATA TO THE SUBJECT SPECIFIC MODEL



(a) The rotational components of the PF joint motion



(b) The translational components of the PF joint motion

Figure 4.12: The experimental motion obtained from the extension movement and the calculated one are shown: the black dashed line is the experimental motion, the red line is the calculated one

between the model and the experimental data is near 1.2 mm for the anterior drawer and 3.1 mm for the posterior. The internal-external rotation reveals a good accuracy, in particular in the external rotation in which the MAE is near 1.5 degrees. A little higher discrepancy is noted in the internal rotation where the mean absolute error is about 2.7 degrees. The ab-adduction test seems the most critical one, the model found a higher stiffness to the varus opening with respect to the reference paper data at every flexion angle except at full extension, on the contrary a higher laxity is noted in response to valgus opening. The mean absolute error are 3.1 and 2.7 degrees for the adduction and the abduction respectively. In Table 4.5 the parameters of the stiffness models before and after the optimization are reported.

Figures 4.14 reports the force that arise in each ligament as function of flexion angle for every test performed. Globally an higher stiffness is noted at full extension than at full flexion in agreement with a common finding in the literature on the physiological behaviour of the knee.

Results show a great contribution of the ACL to the stiffness of the knee in every test. The anterior drawer test (Fig. 4.14 (a)) confirms the role of the ACL as the primary restraint against the anterior tibial translation and internal rotation in accordance to the typical description of the functional role of the this ligament [20]. The importance of the anterior cruciate ligaments in almost all the tests (except for the posterior drawer and external tibial rotation) is related to the mainly vertical orientation of its fibres and to coupled translations and rotations associated to each loading condition.

The PCL ligament confirms to play the most important role in restricting the posterior tibial translation (Fig. 4.14 (b)); it is worth noting that at full extension its contribute is less relevant than in full flexion [2], its importance increases with the flexion angle. On the contrary the PCL is slack in case of anterior tibial displacement (Fig. 4.14 (a)), a minor role is noted also against ab-adduction moments (Fig. 4.14 (c)-(d)).

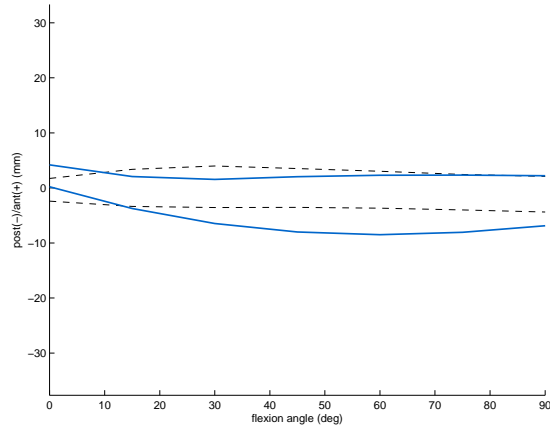
The superficial fibres of MCL reveals to have an active role as a restraint in all the tests except for adduction, in which it exerts a relevant force only at full extension (Fig. 4.14 (c)), probably due to a coupled movement of the tibia. The results confirm it importance against valgus and external rotation torques [12]. Differently the dMCL seems to have a minor role, revealing to be significant only into restraint the external tibial rotations (Fig. 4.14 (f)).

4. FROM IN VIVO CLINICAL DATA TO THE SUBJECT SPECIFIC MODEL

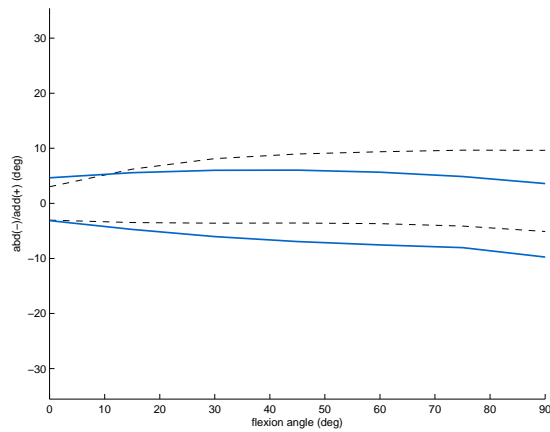
The results of the stiffness models show a minor role of the LCL, which appears slack in almost all the tests and exert some force only against adduction moments (Fig. 4.14 (c)). In the few cases in which it results active, its importance is limited to the first 30 degrees of flexion (Fig. 4.14 (f)) in accordance with the literature [2].

As far as the POL is concerned, results shows its importance as a restraint against valgus rotation, anterior translation and internal rotation (Fig. 4.14 (a)-(d)-(e)). In particular, an increasing relevance of the ligament is noted going towards full flexion. The importance of posterior oblique ligament in valgus opening and internal tibial rotation is confirmed in the literature [12]; however the results partially disagree with those reported in [12], which reports an higher contribute of the POL at full extension than at full flexion.

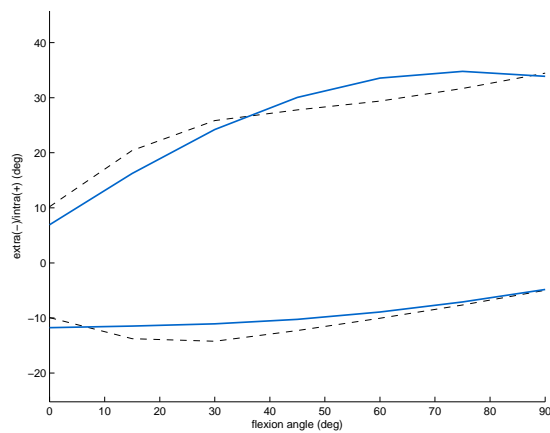
Regarding the popliteus complex, that is to say the PT and the PFL, the model shows how these structures work jointly in most of the cases with the PFL being active when the PT is in tension [2]. The PFL shows a significant role as a secondary restraint to external rotation (Fig. 4.14 (f)), a minor importance is noted also against varus angulation (Fig. 4.14 (d)), posterior translation (Fig. 4.14 (b)) at full extension [42]. As far as the popliteus tendon is concerned, the results confirm its role as a primary restraint against external rotation (Fig. 4.14 (f)) [26], a secondary role is also noted against ab-adduction moments (Fig. 4.14 (c)-(d)) and in anterior-posterior drawer (Fig. 4.14 (a)-(b)).



(a) Results of the anterior/posterior drawer test



(b) Results of the adduction/abduction test



(c) Results of the internal/external rotation test

Figure 4.13: The displacements of the reference paper and the calculated one are shown: the black dashed line is the experimental motion, the blue line is the calculated one

4. FROM IN VIVO CLINICAL DATA TO THE SUBJECT SPECIFIC MODEL

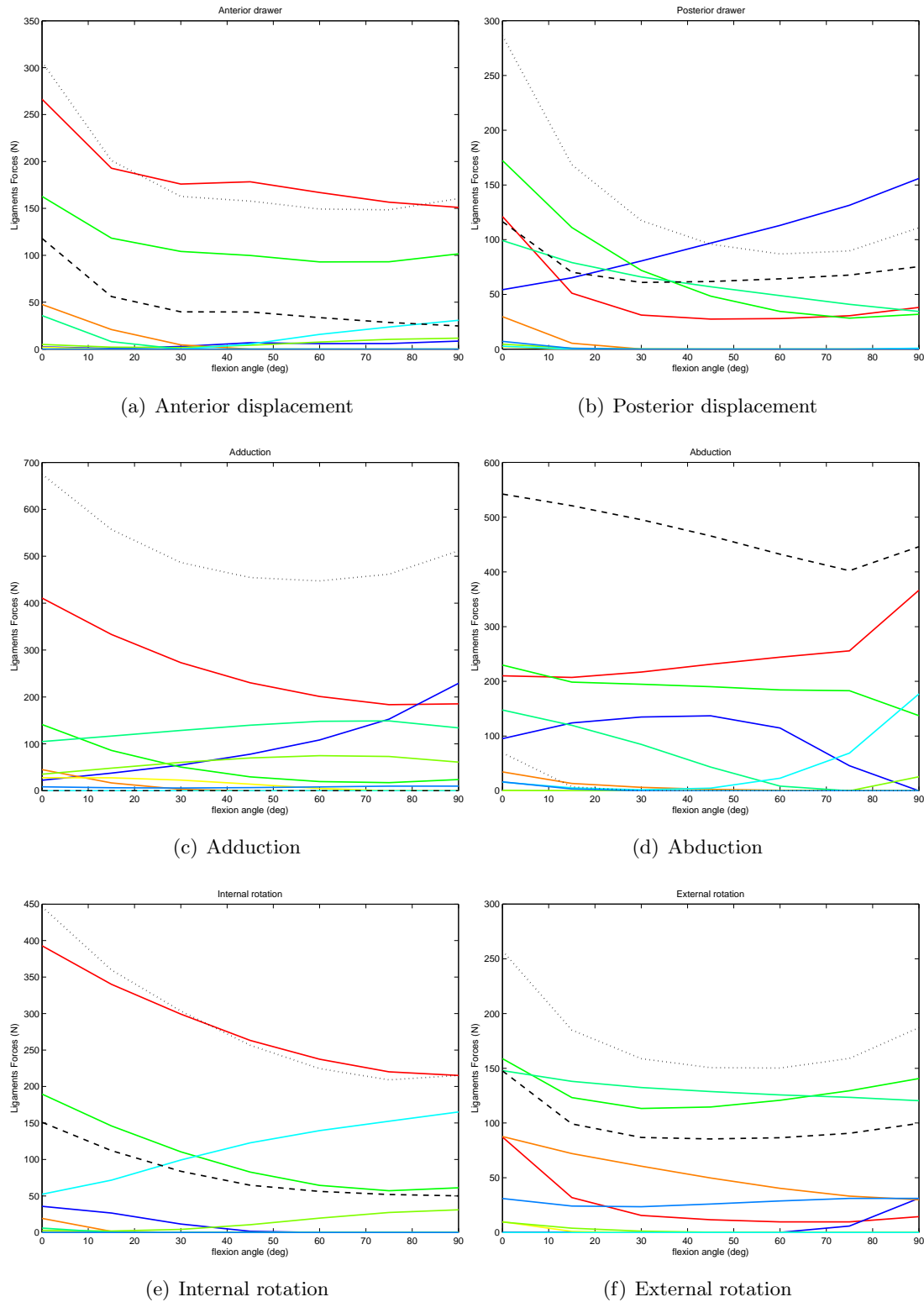


Figure 4.14: Ligaments forces during the clinical tests. ACL (-), PCL(-), sMCL (-), dMCL (-), LCL (-), MLCL (-), PT (-), POL (-), PFL (-), lateral contact (-), medial contact (-)

5

Conclusions

A procedure that allows for the definition of a subject specific knee joint model starting from in vivo clinical data was presented. The detailed procedure stems from data obtained by means of standard computed tomography (CT), magnetic resonance imaging (MRI), and single-plane fluoroscopy on a single subject and leads to the identification of the parameters that define the kinematic and the stiffness models of his knee joint.

A sequential approach to the knee joint modelling, which comprises the definition of the kinematic, stiffness and dynamic models according to certain conditions, was followed. Hence the two models are strictly connected and the kinematic models provides the basis for the stiffness one. Therefore, the kinematic model of the joint was identified at first complete of both the tibio-femoral and the patello-femoral joints, this model was based on the 5-5 parallel mechanism inclusive of the patello-femoral sub-chain. Attention was devoted to the feasibility of the procedure in a standard clinical environment as well as to the anatomical adherence of the identified model to the subject anatomy. In order to enhance this last characteristic of the study, during the process of identification of the parameters of the models, strict boundaries were assumed on all the parameters involved.

The procedure shows a good accuracy, leading to the identification of a model able to accurately replicate the subject specific motion. The experimental motion acquired during the flexion movement was used to obtain the subject specific model of the knee. The identified kinematic model provides a motion that shows great adherence to the experimental motion of the tibio-femoral sub-joint. The motion obtained by the model of the patello-femoral sub-joint shows lower adherence to the experimental one.

5. CONCLUSIONS

Nevertheless, the experimental motion of the PF sub-joint used to obtain the model results affected by uncertainties related to the matching process. With regard to this, an higher adherence is noted between the experimental motion acquired during the knee extension, that appears more reliable, and the motion obtained by the model based on it. The experimental motion acquired during the flexion movement was used for the model of the PF sub-joint in order to have a knee model coherently based on the same movement in both the kinematic and the stiffness part. As far as the identification of the parameters that define the model is concerned, the tight search domain imposed during the identification of the optimized parameters of the model highlights the predictive capabilities of the model. However, a few critical aspects exist that have to be taken into account. Indeed, the use of a single-plane fluroscopy to acquire the experimental motion together with a manually performed registration of the 3-D models on the fluoroscopic images are crucial points. Whereas the use of a single-plane technique leads to the assumption of a lower radiation dose to the patient than the bi-planar one, it has also higher probability of matching error in the components of the motion that lie outside the fluoroscopy plane. The discrepancies between the two methods have to be assessed and the advantages of the bi-planar fluoroscopy in the reconstruction of the motion have to be carefully evaluated and compared with the higher radiation dose absorbed by the patient. As far as the registration procedure, improvements are expected by the implementation of automatic fluoroscopy registration procedures both in terms of increased accuracy and diminished time dedicated to the process.

Regarding the subject specific stiffness model of the joint, the procedure allowed for the determination of the geometry of the model while the identification of the parameters of the stiffness model was based on literature data due to the lack of suitable subject specific data to work with. The procedure led to the definition of a stiffness model that showed good adherence with literature data for almost every loading condition tested. Moreover, the analysis of the forces arising in the ligaments in the considered loading conditions show great adherence with common findings in the literature.

The procedure described in the present study bridges the gap between the usually in vitro defined kinematic and kinetostatic knee joint models and the study of the active structures of the joint which is based on in vivo data. Furthermore, the procedure detailed in the present dissertation is useful for the study and the replication of the

patient specific physiological behaviour of the knee as well as the definition of prosthesis and orthoses personalized on a single patient.

5. CONCLUSIONS

References

- [1] A. M. AHMED AND N. A. DUNCAN. Correlation of patellar tracking pattern with trochlear and retropatellar surface topographies. *Journal of biomechanical engineering*, **122**[December 2000]:652–660, 2000.
- [2] A. A. AMIS, A. M. J. BULL, C. M. GUPTA, I. HJAZI, A. RACE, AND J. R. ROBINSON. Biomechanics of the PCL and related structures: posterolateral, posteromedial and meniscofemoral ligaments. *Knee surgery, sports traumatology, arthroscopy : official journal of the ESSKA*, **11**[5]:271–281, 2003.
- [3] S. A. BANKS AND W. A. HODGE. Accurate measurement of three-dimensional knee replacement kinematics using single-plane fluoroscopy. *IEEE transactions on biomedical engineering*, **43**[6]:638–49, 1996.
- [4] C. BELVEDERE, A. ENSINI, A. FELICIANGELI, F. CENNI, V. D’ANGELI, S. GIANNINI, AND A. LEARDINI. Geometrical changes of knee ligaments and patellar tendon during passive flexion. *Journal of Biomechanics*, **45**[11]:1886–1892, 2012.
- [5] L. BLANKEVOORT, R. HUISKES, AND A. DE LANGE. Helical axes of passive knee joint motions. *Journal of Biomechanics*, **23**:1219–1229, 1990.
- [6] L. BLANKEVOORT, J. H. KUIPER, R. HUISKES, AND H. J. GROOTENBOER. Articular contact in a three-dimensional model of the knee. *Journal of Biomechanics*, **24**[2]:1019–1031, 1991.
- [7] N. V. BOLOG, G. ANDREISEK, AND E. J. ULBRICH. *MRI of the Knee*. Springer International Publishing, 2015.
- [8] J.-M. BRINKMAN, P. J. A. SCHWERING, L. BLANKEVOORT, J. G. KOOLOOS, J. LUITES, AND A. B. WYMENGA. The insertion geometry of the posterolateral corner of the knee. *The Journal of bone and joint surgery. British volume*, **87**[10]:1364–8, 2005.
- [9] F. FREUDENSTEIN AND L.S. WOO. Kinematics of the human knee. *Bulletin of mathematical biophysics*, **31**, 1969.
- [10] F. K. FUSS. Anatomy of the cruciate ligaments and their function in extension and flexion of the human knee joint. *The American journal of anatomy*, **184**[2]:165–176, 1989.
- [11] F. G. GIRGIS, J. L. MARSHALL, AND A. R. S. A. MONAJEM. The cruciate ligaments of the knee joint: Anatomical, functional and experimental analysis. *Clinical Orthopaedics & Related Research*, **106**:216–231, January/February 1975.
- [12] C. J. GRIFFITH, C. A. WIJCKICKS, R. F. LAPRADE, B. M. ARMITAGE, S. JOHANSEN, AND L. ENGBRETSSEN. Force Measurements on the Posterior Oblique Ligament and Superficial Medial Collateral Ligament Proximal and Distal Divisions to Applied Loads. *The American Journal of Sports Medicine*, **37**[1]:140–148, 2010.
- [13] E. S. GROOD, S. F. STOWERS, AND F. R. NOYES. Limits of movement in the human knee. Effect of sectioning the posterior cruciate ligament and posterolateral structures. *The Journal of bone and joint surgery. American volume*, **70**[1]:88–97, 1988.
- [14] E. S. GROOD AND W. J. SUNTAY. A joint coordinate system for the clinical description of three-dimensional motions: application to the knee. *Journal of biomechanical engineering*, 1983.
- [15] C. D. HARNER, G. H. BAEK, T. M. VOGRIN, G. J. CARLIN, S. KASHIWAGUCHI, AND S. L. WOO. Quantitative analysis of human cruciate ligament insertions. *Arthroscopy*, **15**[7]:741–749, 1999.
- [16] G. HEE JUNG, J. DO KIM, AND H. KIM. Location and classification of popliteus tendon’s origin: cadaveric study. *Arch Orthop Trauma Surg*, **130**:1027–1032, 2010.
- [17] J. HEEGAARD, P. F. LEYVRAZ, A. CURNIER, L. RAKOTOMANANA, AND R. HUISKES. The biomechanics of the human patella during passive knee flexion. *J Biomech*, **28**[11]:1265–1279, Nov 1995.
- [18] M. S. HEFZY AND T. DEREK V. COOKE. Review of knee models: 1996 update. *Applied Mechanics Reviews*, **49**[10S]:S187–S193, October 1996.
- [19] M. S. HEFZY AND E. S. GROOD. Review of Knee Models. *Applied Mechanics Reviews*, **41**[1]:1–13, 1988.
- [20] A. KANAMORI, S. L.-Y. WOO, C. BENJAMIN MA, J. ZEMINSKI, T. W. RUDY, G. LI, AND GLEN A. LIVESAY. The forces in the anterior cruciate ligament and knee kinematics during a simulated pivot shift test: A human cadaveric study using robotic technology. *Arthroscopy*, **16**[6]:633–639, 2000.
- [21] S. KOPF, V. MUSAHL, S. TASHMAN, M. SZCZODRY, W. SHEN, AND F. H. FU. A systematic review of the femoral origin and tibial insertion morphology of the ACL. *Knee Surgery, Sports Traumatology, Arthroscopy*, **17**[3]:213–219, 2009.
- [22] R. F. LAPRADE. Mechanical Properties of the Posterolateral Structures of the Knee. *American Journal of Sports Medicine*, **33**[9]:1386–1391, 2005.
- [23] R. F. LAPRADE. The Anatomy of the Medial Part of the Knee. *The Journal of Bone and Joint Surgery (American)*, **89**[9]:2000, 2007.
- [24] R. F. LAPRADE, T. J. GILBERT, T. S. BOLLUM, F. WENTORF, AND G. CHALJUB. The magnetic resonance imaging appearance of individual structures of the posterolateral knee. A prospective study of normal knees and knees with surgically verified grade III injuries. *The American journal of sports medicine*, **28**[2]:191–199, 2000.
- [25] R. F. LAPRADE, T. V. LY, F. A. WENTORF, AND L. ENGBRETSSEN. The posterolateral attachments of the knee: a qualitative and quantitative morphologic analysis of the fibular collateral ligament, popliteus tendon, popliteofibular ligament, and lateral gastrocnemius tendon. *The American journal of sports medicine*, **31**[6]:854–860, 2003.

REFERENCES

- [26] R. F. LAPRADE, J. K. WOZNICZKA, M. P. STELLMAKER, AND C. A. WIDDICKS. Analysis of the static function of the popliteus tendon and evaluation of an anatomic reconstruction: the "fifth ligament" of the knee. *The American journal of sports medicine*, **38**[3]:543–549, 2010.
- [27] F. LIU, B. YUE, H. R. GADIKOTA, M. KOZANEK, W. LIU, T. J. GILL, H. E. RUBASH, AND G. LI. Morphology of the medial collateral ligament of the knee. *Journal of orthopaedic surgery and research*, **5**:69, 2010.
- [28] R. LOREDO, J. HODLER, R. PEDOWITZ, L. R. YEH, D. TRUDELL, AND D. RESNICK. Posteromedial corner of the knee: MR imaging with gross anatomic correlation. *Skeletal Radiology*, **28**[6]:305–311, 1999.
- [29] M. A. MARRA, V. VANHEULE, R. FLUIT, B. H. F. J. M. KOOPMAN, J. RASMUSSEN, N. VERDONSCHOT, AND M. S. ANDERSEN. A subject-specific musculoskeletal modeling framework to predict in vivo mechanics of total knee arthroplasty. *Journal of Biomechanical Engineering*, **137**[2]:020904–020904, February 2015.
- [30] T. J. MOMMERSTEEG, L. BLANKEVOORT, R. HUISKES, J. G. KOOLOOS, AND J. M. KAUER. Characterization of the mechanical behavior of human knee ligaments: a numerical-experimental approach. *Journal of biomechanics*, **29**[2]:151–160, 1996.
- [31] T. J. MOMMERSTEEG, R. HUISKES, L. BLANKEVOORT, J. G. KOOLOOS, J. M. KAUER, AND G. M. MAATHUIS. A global verification study of a quasi-static knee model with multi-bundle ligaments. *Journal of Biomechanics*, **29**[12]:1659–1664, 1996.
- [32] T. J. MOMMERSTEEG, J. G. KOOLOOS, L. BLANKEVOORT, J. M. KAUER, R. HUISKES, AND F. Q. ROELING. The fibre bundle anatomy of human cruciate ligaments. *Journal of anatomy*, **187** (Pt 2):461–471, 1995.
- [33] A. OTTOBONI, V. PARENTI-CASTELLI, N. SANCISI, C. BELVEDERE, AND A. LEARDINI. Articular surface approximation in equivalent spatial parallel mechanism models of the human knee joint: an experiment-based assessment. *Proceedings of the Institution of Mechanical Engineers, Part H: Journal of Engineering in Medicine*, **224**[9]:1121–1132, sep 2010.
- [34] V. PARENTI-CASTELLI AND R. GREGORIO. Parallel mechanisms applied to the human knee passive motion simulation. In *Advances in Robot Kinematics*, pages 333–344. Dordrecht, 2000. Springer Netherlands.
- [35] V. PARENTI-CASTELLI, A. LEARDINI, R. DI GREGORIO, AND J. J. O'CONNOR. On the modeling of passive motion of the human knee joint by means of equivalent planar and spatial parallel mechanisms. *Autonomous Robots*, **16**[2]:219–232.
- [36] J. R. ROBINSON, A. M. J. BULL, AND A. A. AMIS. Structural properties of the medial collateral ligament complex of the human knee. *Journal of Biomechanics*, **38**[5]:1067–1074, 2005.
- [37] J. R. ROBINSON, J. SANCHEZ-BALLESTER, A. M. J. B., R. DE W. M. THOMAS, AND A. A. AMIS. The posteromedial corner revisited. *The Journal of Bone and Joint Surgery*, **86**[5]:674–681, 2004.
- [38] J. S. ROVICK, J. D. REUBEN, R. J. SCHRAGER, AND P. S. WALKER. Relation between knee motion and ligament length patterns. *Clinical Biomechanics*, **6**[4]:213–220, 1991.
- [39] N. SANCISI AND V. PARENTI-CASTELLI. A 1-Dof parallel spherical wrist for the modelling of the knee passive motion. *Mechanism and Machine Theory*, **45**[4]:658–665, apr 2010.
- [40] N. SANCISI AND V. PARENTI-CASTELLI. A novel 3D parallel mechanism for the passive motion simulation of the patella-femur-tibia complex. *Meccanica*, **46**:207–220, 2011.
- [41] N. SANCISI AND V. PARENTI-CASTELLI. A sequentially-defined stiffness model of the knee. *Mechanism and Machine Theory*, **46**[12]:1920–1928, dec 2011.
- [42] S. A. SHAHANE, C. IBBOTSON, R. STRACHAN, AND D. R. BICKERSTAFF. The popliteofibular ligament. An anatomical study of the posterolateral corner of the knee. *The Journal of bone and joint surgery. British volume*, **81**[4]:636–642, 1999.
- [43] H. STRASSER. *Lehrbuch der Muskel und Gelenkmechanik*. Springer Berlin, 1917.
- [44] Y. TANAKA, Y. SHIOZAKI, Y. YONETANI, T. KANAMOTO, A. TSUJII, AND S. HORIBE. Mri analysis of the attachment of the anteromedial and posterolateral bundles of anterior cruciate ligament using coronal oblique images. *Knee Surgery, Sports Traumatology, Arthroscopy*, **19**[1]:54–59, 2011.
- [45] C. A. WIDDICKS, D. T. EWART, D. J. NUCKLEY, S. JOHANSEN, L. ENGBRETSSEN, AND ROBERT F. LAPRADE. Structural properties of the primary medial knee ligaments. *The American journal of sports medicine*, **38**[8]:1638–1646, 2010.
- [46] D. R. WILSON, J. D. FEIKES, A. B. ZAVATSKY, AND J. J. O'CONNOR. The components of passive knee movement are coupled to flexion angle. *Journal of biomechanics*, **33**[4]:465–473, 2000.
- [47] D. R. WILSON AND J. J. O'CONNOR. A three-dimensional geometric model of the knee for the study of joint forces in gait. *Gait and Posture*, **5**:108–115, 1997.
- [48] A. WING HUNG NG, J. F. GRIFFITH, K. YIP LAW, J. W. M. TING, G. L. TIPOE, A. T. AHUJA, AND K. MING CHAN. Oblique axial MR imaging of the normal anterior cruciate ligament bundles. *Skeletal Radiology*, **40**[12]:1587–1594, 2011.
- [49] G. WU AND P. R. CAVANAGH. ISB Recommendations in the Reporting for Standardization of Kinematic Data. *Journal of Biomechanics*, **28**[10]:1257–1261, 1995.
- [50] P. A. YUSHKEVICH, J. PIVEN, H. CODY HAZLETT, R. GIMPEL SMITH, S. HO, J. C. GEE, AND G. GERIG. User-guided 3D active contour segmentation of anatomical structures: Significantly improved efficiency and reliability. *Neuroimage*, **31**[3]:1116–1128, 2006.